Functional quantization of rough volatility and applications to volatility derivatives

O. Bonesini, G. Callegaro & A. Jacquier

Published online: 03 Dec 2023.

Submit your article to this journal ⬈

View related articles ⬈

View Crossmark data ⬈

Routledge
Taylor & Francis Group

Check for updates

Functional quantization of rough volatility and applications to volatility derivatives

O. BONESINI†, G. CALLEGARO ⓘ*† and A. JACQUIER‡

†Dipartimento di Matematica, "T. Levi-Civita", Via Trieste. 63, Padova 35121, Italy
‡Department of Mathematics, Imperial College London, London SW7 1NE, UK

We develop a product functional quantization of rough volatility. Since the optimal quantizers can be computed offline, this new technique, built on the insightful works by [Luschgy, H. and Pagès, G., Functional quantization of Gaussian processes. *J. Funct. Anal.*, 2002, **196**(2), 486–531; Luschgy, H. and Pagès, G., High-resolution product quantization for Gaussian processes under sup-norm distortion. *Bernoulli*, 2007, **13**(3), 653–671; Pagès, G., Quadratic optimal functional quantization of stochastic processes and numerical applications. In *Monte Carlo and Quasi-Monte Carlo Methods 2006*, pp. 101–142, 2007 (Springer: Berlin Heidelberg)], becomes a strong competitor in the new arena of numerical tools for rough volatility. We concentrate our numerical analysis on the pricing of options on the VIX and realized variance in the rough Bergomi model [Bayer, C., Friz, P.K. and Gatheral, J., Pricing under rough volatility. *Quant. Finance*, 2016, **16**(6), 887–904] and compare our results to other benchmarks recently suggested.

Keywords: Riemann–Liouville process; Volterra process; Functional quantization; Series expansion; Rough volatility; Vix options

1. Introduction

Gatheral *et al.* (2018) recently introduced a new framework for financial modelling. To be precise—according to the reference website https://sites.google.com/site/roughvol/home— almost 2400 days have passed since instantaneous volatility was shown to have a rough nature, in the sense that its sample paths are α-Hölder-continuous with $\alpha < \frac{1}{2}$. Many studies, both empirical (Bennedsen *et al.* 2017, Fukasawa 2021, Fukasawa *et al.* 2022) and theoretical (Alòs *et al.* 2007, Fukasawa 2011), have confirmed this, showing that these so-called rough volatility models are a more accurate fit to the implied volatility surface and to estimate historical volatility time series.

On equity markets, the quality of a model is usually measured by its ability to calibrate not only to the SPX implied volatility but also VIX Futures and the VIX implied volatility. The market standard models had so far been Markovian, in particular the double mean-reverting process (Gatheral 2008, Huh *et al.* 2018), Bergomi's model (Bergomi 2005) and, to some extent, jump models (Carr and Madan 2014, Kokholm and Stisen 2015). However, they each suffer from several drawbacks, which the new generation of rough volatility models seems to overcome. For VIX Futures pricing, the rough version of Bergomi's model was thoroughly investigated in Jacquier *et al.* (2018a), showing accurate results. Nothing comes for free though and the new challenges set by rough volatility models lie on the numerical side, as new tools are needed to develop fast and accurate numerical techniques. Since classical simulation tools for fractional Brownian motions are too slow for realistic purposes, new schemes have been proposed to speed it up, among which the Monte Carlo hybrid scheme (Bennedsen *et al.* 2017, McCrickerd and Pakkanen 2018), a tree formulation (Horvath *et al.* 2019), quasi Monte-Carlo methods (Bayer *et al.* 2020) and Markovian approximations (Abi Jaber and El Euch 2019, Chen *et al.* 2021).

We suggest here a new approach, based on product functional quantization (Pagès 2007). Quantization was originally conceived as a discretization technique to approximate a continuous signal by a discrete one (Sheppard 1897), later developed at Bell Laboratory in the 1950s for signal transmission (Gersho and Gray 1992). It was, however, only in the 1990s that its power to compute (conditional) expectations of functionals of random variables (Graf and Luschgy 2007) was fully understood. Given an $\mathbb{R}^d$-valued random vector on some probability space, optimal vector quantization investigates how to select an $\mathbb{R}^d$-valued random vector $\widehat{X}$, supported

*Corresponding author. Email: gcallega@math.unipd.it

on at most N elements, that best approximates X according to a given criterion (such as the L^r-distance, $r \geq 1$). Functional quantization is the infinite-dimensional version, approximating a stochastic process with a random vector taking a finite number of values in the space of trajectories for the original process. It has been investigated precisely (Luschgy and Pagès 2002, Pagès 2007) in the case of Brownian diffusions, in particular for financial applications (Pagès and Printems 2005). However, optimal functional quantizers are in general hard to compute numerically and instead product functional quantizers provide a rate-optimal (so, in principle, sub-optimal) alternative often admitting closed-form expressions (Pagès and Printems 2005, Luschgy and Pagès 2007).

In section 2, we briefly review important properties of *Gaussian Volterra processes*, displaying a series expansion representation, and paying special attention to the *Riemann–Liouville* case in section 2.2. This expansion yields, in section 3, a product functional quantization of the processes, that shows an L^2-error of order $\log(N)^{-H}$, with N the number of paths and H a regularity index. We then show, in section 3.1, that these functional quantizers, although sub-optimal, are stationary. We specialize our setup to the generalized rough Bergomi model in section 4 and show how product functional quantization applies to the pricing of VIX Futures and VIX options, proving in particular precise rates of convergence. Finally, section 5 provides a numerical confirmation of the quality of our approximations for VIX Futures and Call Options on the VIX in the rough Bergomi model, benchmarked against other existing schemes. In this section, we also discuss how product functional quantization of the Riemann–Liouville process itself can be exploited to price options on realized variance.

Notations   We set $\mathbb{N}$ as the set of strictly positive natural numbers. We denote by $\mathcal{C}[0,1]$ the space of real-valued continuous functions over $[0,1]$ and by $L^2[0,1]$ the Hilbert space of real-valued square integrable functions on $[0,1]$, with inner product $\langle f, g \rangle_{L^2[0,1]} := \int_0^1 f(t)g(t)\,\mathrm{d}t$, inducing the norm $\|f\|_{L^2[0,1]} := (\int_0^1 |f(t)|^2\,\mathrm{d}t)^{1/2}$, for each $f, g \in L^2[0,1]$. $L^2(\mathbb{P})$ denotes the space of square integrable (with respect to $\mathbb{P}$) random variables.

2. Gaussian Volterra processes on $\mathbb{R}_+$

For clarity, we restrict ourselves to the time interval $[0,1]$. Let $\{W_t\}_{t\in[0,1]}$ be a standard Brownian motion on a filtered probability space $(\Omega, \mathcal{F}, \{\mathcal{F}_t\}_{t\in[0,1]}, \mathbb{P})$, with $\{\mathcal{F}_t\}_{t\in[0,1]}$ its natural filtration. On this probability space, we introduce the Volterra process

$$Z_t := \int_0^t K(t-s)\,\mathrm{d}W_s, \quad t \in [0,1], \tag{1}$$

and we consider the following assumptions for the kernel K:

ASSUMPTION 2.1 There exist $\alpha \in (-\frac{1}{2}, \frac{1}{2}) \setminus \{0\}$ and $L : (0,1] \to (0,\infty)$ continuously differentiable, slowly varying at 0, that is, for any $t > 0$, $\lim_{x\downarrow 0} \frac{L(tx)}{L(x)} = 1$, and bounded away from 0 function with $|L'(x)| \leq C(1 + x^{-1})$, for $x \in (0,1]$, for

some $C > 0$, such that

$$K(x) = x^\alpha L(x), \quad x \in (0,1].$$

This implies in particular that $K \in L^2[0,1]$, so that the stochastic integral (1) is well defined. The Gamma kernel, with $K(u) = e^{-\beta u}u^\alpha$, for $\beta > 0$ and $\alpha \in (-\frac{1}{2}, \frac{1}{2}) \setminus \{0\}$, is a classical example satisfying assumption 2.1. Straightforward computations show that the covariance function of Z reads

$$R_Z(s,t) = \int_0^{t\wedge s} K(t-u)K(s-u)\,\mathrm{d}u, \quad s,t \in [0,1].$$

Under assumption 2.1, Z is a Gaussian process admitting a version which is ε-Hölder continuous for any $\varepsilon < \frac{1}{2} + \alpha = H$ and hence also admits a continuous version (Bennedsen *et al.* 2017, Proposition 2.11).

2.1. Series expansion

We introduce a series expansion representation for the centered Gaussian process Z in (1), which will be key to develop its functional quantization. Inspired by Luschgy and Pagès (2007), introduce the stochastic process

$$Y_t := \sum_{n\geq 1} \mathcal{K}[\psi_n](t)\xi_n, \quad t \in [0,1], \tag{2}$$

where $\{\xi_n\}_{n\geq 1}$ is a sequence of i.i.d. standard Gaussian random variables, $\{\psi_n\}_{n\geq 1}$ denotes the orthonormal basis of $L^2[0,1]$:

$$\psi_n(t) = \sqrt{2}\cos\left(\frac{t}{\sqrt{\lambda_n}}\right), \quad \text{with } \lambda_n = \frac{4}{(2n-1)^2\pi^2}, \tag{3}$$

and the operator $\mathcal{K} : L^2[0,1] \to \mathcal{C}[0,1]$ is defined for $f \in L^2[0,1]$ as

$$\mathcal{K}[f](t) := \int_0^t K(t-s)f(s)\,\mathrm{d}s, \quad \text{for all } t \in [0,1]. \tag{4}$$

REMARK 2.2 The stochastic process Y in (2) is defined as a weighted sum of independent centered Gaussian variables, so for every $t \in [0,1]$ the random variable Y_t is a centered Gaussian random variable and the whole process Y is Gaussian with zero mean.

We set the following assumptions on the functions $\{\mathcal{K}[\psi_n]\}_{n\in\mathbb{N}}$:

ASSUMPTION 2.3 There exists $H \in (0, \frac{1}{2})$ such that

(A) there is a constant $C_1 > 0$ for which, for any $n \geq 1$, $\mathcal{K}[\psi_n]$ is $(H + \frac{1}{2})$-Hölder continuous, with

$$\sup_{s,t\in[0,1],s\neq t} \frac{|\mathcal{K}[\psi_n](t) - \mathcal{K}[\psi_n](s)|}{|t-s|^{H+\frac{1}{2}}} \leq C_1 n;$$

(B) there exists a constant $C_2 > 0$ such that

$$\sup_{t\in[0,1]} |\mathcal{K}[\psi_n](t)| \leq C_2 n^{-(H+\frac{1}{2})}, \quad \text{for all } n \geq 1.$$

Note that under these assumptions, the series (2) converges both almost surely and in $L^2(\mathbb{P})$ for each $t \in [0, 1]$ by Khintchine–Kolmogorov Convergence Theorem (Chow and Teichner 1997, theorem 1, section 5.1).

It is natural to wonder whether assumption 2.1 implies assumption 2.3 given the basis functions (3). This is far from trivial in our general setup and we provide examples and justifications later on for models of interest. Similar considerations with slightly different conditions can be found in Luschgy and Pagès (2007). We now focus on the variance–covariance structure of the Gaussian process Y.

LEMMA 2.4 *For any $s, t \in [0, 1]$, the covariance function of Y is given by*

$$R_Y(s, t) := \mathbb{E}[Y_s Y_t] = \int_0^{t \wedge s} K(t - u) K(s - u) \, \mathrm{d}u.$$

Proof Exploiting the definition of Y in (2), the definition of $\mathcal{K}$ in (4) and the fact that the random variable ξ_n's are i.i.d. standard Normal, we obtain

$$R_Y(s, t) = \mathbb{E}[Y_s Y_t] = \mathbb{E}\left[\left(\sum_{n \geq 1} \mathcal{K}[\psi_n](s)\xi_n\right)\right.$$
$$\times \left.\left(\sum_{m \geq 1} \mathcal{K}[\psi_m](t)\xi_m\right)\right]$$
$$= \sum_{n \geq 1} \mathcal{K}[\psi_n](s)\mathcal{K}[\psi_n](t)$$
$$= \sum_{n \geq 1} \left(\int_0^1 K(s - u)\mathbf{1}_{[0,s]}(u)\psi_n(u) \, \mathrm{d}u\right.$$
$$\times \left.\int_0^1 K(t - r)\mathbf{1}_{[0,t]}(r)\psi_n(r) \, \mathrm{d}r\right)$$
$$= \sum_{n \geq 1} \langle K(s - \cdot)\mathbf{1}_{[0,s]}(\cdot), \psi_n \rangle_{L^2[0,1]}$$
$$\cdot \langle K(t - \cdot)\mathbf{1}_{[0,t]}(\cdot), \psi_n \rangle_{L^2[0,1]}$$
$$= \sum_{n \geq 1} \Big\langle K(t - \cdot)\mathbf{1}_{[0,t]}(\cdot),$$
$$\langle K(s - \cdot)\mathbf{1}_{[0,s]}(\cdot), \psi_n \rangle_{L^2[0,1]}\psi_n \Big\rangle_{L^2[0,1]}$$
$$= \Big\langle K(t - \cdot)\mathbf{1}_{[0,t]}(\cdot), \sum_{n \geq 1} \langle K(s - \cdot)$$
$$\times \mathbf{1}_{[0,s]}(\cdot), \psi_n \rangle_{L^2[0,1]}\psi_n \Big\rangle_{L^2[0,1]}$$
$$= \langle K(t - \cdot)\mathbf{1}_{[0,t]}(\cdot), K(s - \cdot)\mathbf{1}_{[0,s]}(\cdot) \rangle_{L^2[0,1]}$$
$$= \int_0^1 K(s - u)\mathbf{1}_{[0,s]}(u)K(t - u)\mathbf{1}_{[0,t]}(u) \, \mathrm{d}u$$
$$= \int_0^{t \wedge s} K(t - u)K(s - u) \, \mathrm{d}u. \blacksquare$$

REMARK 2.5 Note that the centered Gaussian stochastic process Y admits a continuous version, too. Indeed, we have

shown that Y has the same mean and covariance function as Z and, consequently, that the increments of the two processes share the same distribution. Thus Bennedsen *et al.* (2017, proposition 2.11) applies to Y as well, yielding that the process admits a continuous version. This last key property of Y can be alternatively proved directly as done in appendix A.2.

Lemma 2.4 implies that $\mathbb{E}[Y_s Y_t] = \mathbb{E}[Z_s Z_t]$, for all $s, t \in [0, 1]$. Both Z and Y are continuous, centered, Gaussian with the same covariance structure, so from now on we will work with Y, using

$$Z = \sum_{n \geq 1} \mathcal{K}[\psi_n]\xi_n, \quad \mathbb{P}-\text{a.s.} \tag{5}$$

2.2. The Riemann–Liouville case

For $K(u) = u^{H - \frac{1}{2}}$, with $H \in (0, \frac{1}{2})$, the process (1) takes the form

$$Z_t^H := \int_0^t (t - s)^{H - \frac{1}{2}} \, \mathrm{d}W_s, \quad t \in [0, 1],$$

where we add the superscript H to emphasize its importance. It is called a *Riemann–Liouville process* (henceforth RL) (also known as *Type II fractional Brownian motion* or *Lévy fractional Brownian motion*), as it is obtained by applying the Riemann–Liouville fractional operator to the standard Brownian motion, and is an example of a Volterra process. This process enjoys properties similar to those of the fractional Brownian motion (fBM), in particular being H-self-similar and centered Gaussian. However, contrary to the fractional Brownian motion, its increments are not stationary. For a more detailed comparison between the fBM and Z^H, we refer to Picard (2011, theorem 5.1). In the RL case, the covariance function $R_{Z^H}(\cdot, \cdot)$ is available (Jacquier *et al.* 2018b, proposition 2.1) explicitly as

$$R_{Z^H}(s, t) = \frac{1}{H + \frac{1}{2}}(s \wedge t)^{H + \frac{1}{2}}(s \vee t)^{H - \frac{1}{2}}$$
$$\times {}_2F_1\left(1, \frac{1}{2} - H; 2H + 1; \frac{s \wedge t}{s \vee t}\right), \quad s, t \in [0, 1],$$

where ${}_2F_1(a, b; c; z)$ denotes the Gauss hypergeometric function (Olver 1997, chapter 5, section 9). More generally, Olver (1997, chapter 5, Section 11), the generalized hypergeometric functions ${}_pF_q(z)$ are defined as

$${}_pF_q(z) = {}_pF_q(a_1, a_2, - - \ldots, a_p; c_1, c_2, \ldots, c_q; z)$$
$$:= \sum_{k=0}^{\infty} \frac{(a_1)_k (a_2)_k \cdots (a_p)_k}{(c_1)_k (c_2)_k \ldots (c_q)_k} \frac{z}{k!}, \tag{6}$$

with the Pochammer's notation $(a)_0 := 1$ and $(a)_k := a(a + 1)(a + 2) \cdots (a + k - 1)$, for $k \geq 1$, where none of the c_k are negative integers or zero. For $p \leq q$ the series (6) converges for all z and when $p = q + 1$ convergence holds for $|z| < 1$ and the function is defined outside this disk by analytic continuation. Finally, when $p > q + 1$ the series diverges for nonzero z unless one of the a_k's is zero or a negative integer.

Regarding the series representation (2), we have, for $t \in [0,1]$ and $n \geq 1$,

$$
\mathcal{K}_H[\psi_n](t):
$$
$$
= \sqrt{2} \int_0^t (t-s)^{H-\frac{1}{2}} \cos\left(\frac{s}{\sqrt{\lambda_n}}\right) \mathrm{d}s
$$
$$
= \frac{2\sqrt{2}}{1+2H} t^{H+\frac{1}{2}} {}_1F_2\left(1; \frac{3}{4}+\frac{H}{2}, \frac{5}{4}+\frac{H}{2}; -\frac{t^2}{4\lambda_n}\right). \quad (7)
$$

Assumption 2.3 holds in the RL case here using (Luschgy and Pagès 2007, lemma 4) (identifying $\mathcal{K}_H[\psi_n]$ to f_n from Luschgy and Pagès (2007, equation (3.7))). Assumption 2.3 (B) implies that, for all $t \in [0,1]$,

$$
\sum_{n \geq 1} \mathcal{K}_H[\psi_n](t)^2 \leq \sum_{n \geq 1} \left(\sup_{t \in [0,1]} |\mathcal{K}_H[\psi_n](t)|\right)^2
$$
$$
\leq C_2^2 \sum_{n \geq 1} \frac{1}{n^{1+2H}} < \infty,
$$

and therefore the series (2) converges both almost surely and in $L^2(\mathbb{P})$ for each $t \in [0,1]$ by Khintchine–Kolmogorov Convergence Theorem (Chow and Teichner 1997, theorem 1, section 5.1).

REMARK 2.6 The expansion (2) is in general not a Karhunen–Loève decomposition (Pagès and Printems 2005, section 4.1.1). In the RL case, it can be numerically checked that the basis $\{\mathcal{K}_H[\psi_n]\}_{n \in \mathbb{N}}$ is not orthogonal in $L^2[0,1]$ and does not correspond to eigenvectors for the covariance operator of the Riemann–Liouville process. In his PhD Thesis (Corlay 2011), Corlay exploited a numerical method to obtain approximations of the first terms in the K–L expansion of processes for which an explicit form is not available.

3. Functional quantization and error estimation

Optimal (quadratic) vector quantization was conceived to approximate a square integrable random vector $X : (\Omega, \mathcal{F}, \mathbb{P}) \to \mathbb{R}^d$ by another one $\widehat{X}$, taking at most a finite number N of values, on a grid $\Gamma^N := \{x_1^N, x_2^N, \ldots, x_N^N\}$, with $x_i^N \in \mathbb{R}^d, i = 1, \ldots, N$. The quantization of X is defined as $\widehat{X} := \mathrm{Proj}_{\Gamma^N}(X)$, where $\mathrm{Proj}_{\Gamma^N} : \mathbb{R}^d \to \Gamma^N$ denotes the nearest neighbor projection. Of course the choice of the N-quantizer Γ^N is based on a given optimality criterion: in most cases Γ^N minimizes the distance $\mathbb{E}[|X - \widehat{X}|^2]^{1/2}$. We recall basic results for one-dimensional standard Gaussian, which shall be needed later, and refer to Graf and Luschgy (2007) for a comprehensive introduction to quantization.

DEFINITION 3.1 Let ξ be a one-dimensional standard Gaussian on a probability space $(\Omega, \mathcal{F}, \mathbb{P})$. For each $n \in \mathbb{N}$, we define the *optimal quadratic n-quantization of ξ* as the random variable $\widehat{\xi}^n := \mathrm{Proj}_{\Gamma^n}(\xi) = \sum_{i=1}^n x_i^n 1_{C_i(\Gamma^n)}(\xi)$, where $\Gamma^n = \{x_1^n, \ldots, x_n^n\}$ is the unique optimal quadratic n-quantizer

of ξ, namely the unique solution to the minimization problem

$$
\min_{\Gamma^n \subset \mathbb{R}, \mathrm{Card}(\Gamma^n)=n} \mathbb{E}[|\xi - \mathrm{Proj}_{\Gamma^n}(\xi)|^2],
$$

and $\{C_i(\Gamma^n)\}_{i \in \{1, \ldots, n\}}$ is a Voronoi partition of $\mathbb{R}$, that is a Borel partition of $\mathbb{R}$ that satisfies

$$
C_i(\Gamma^n) \subset \left\{ y \in \mathbb{R} : |y - x_i^n| = \min_{1 \leq j \leq n} |y - x_j^n| \right\} \subset \overline{C}_i(\Gamma^n),
$$

where the right-hand side denotes the closure of the set in $\mathbb{R}$.

The unique optimal quadratic n-quantizer $\Gamma^n = \{x_1^n, \ldots, x_n^n\}$ and the corresponding quadratic error are available online, at http://www.quantize.maths-fi.com/gaussian_database for $n \in \{1, \ldots, 5999\}$.

Given a stochastic process, viewed as a random vector taking values in its trajectories space, such as $L^2[0,1]$, functional quantization does the analogue to vector quantization in an infinite-dimensional setting, approximating the process with a finite number of trajectories. In this section, we focus on product functional quantization of the centered Gaussian process Z from (1) of order N (see Pagès 2007, section 7.4 for a general introduction to product functional quantization). Recall that we are working with the continuous version of Z in the series (5). For any $m, N \in \mathbb{N}$, we introduce the following set, which will be of key importance all throughout the paper:

$$
\mathcal{D}_m^N := \left\{ \mathbf{d} \in \mathbb{N}^m : \prod_{i=1}^m d(i) \leq N \right\}. \quad (8)
$$

DEFINITION 3.2 A *product functional quantization of Z of order N* is defined as

$$
\widehat{Z}_t^{\mathbf{d}} := \sum_{n=1}^m \mathcal{K}[\psi_n](t) \widehat{\xi}_n^{d(n)}, \quad t \in [0,1], \quad (9)
$$

where $\mathbf{d} \in \mathcal{D}_m^N$, for some $m \in \mathbb{N}$, and for every $n \in \{1, \ldots, m\}$, $\widehat{\xi}_n^{d(n)}$ is the (unique) optimal quadratic quantization of the standard Gaussian random variable ξ_n of order $d(n)$, according to definition 3.1.

REMARK 3.3 The condition $\prod_{i=1}^m d(i) \leq N$ in equation (8) motivates the wording 'product' functional quantization. Clearly, the optimality of the quantizer also depends on the choice of m and $\mathbf{d}$, for which we refer to proposition 3.6 and section 5.1.

Before proceeding, we need to make precise the explicit form for the product functional quantizer of the stochastic process Z:

DEFINITION 3.4 The *product functional $\mathbf{d}$-quantizer of Z* is defined as

$$
\chi_{\underline{i}}^{\mathbf{d}}(t) := \sum_{n=1}^m \mathcal{K}[\psi_n](t) \, x_{i_n}^{d(n)}, \quad t \in [0,1], \, \underline{i} = (i_1, \ldots, i_m),
$$

for $\mathbf{d} \in \mathcal{D}_m^N$ and $1 \leq i_n \leq d(n)$ for each $n = 1, \ldots, m$.

REMARK 3.5 Intuitively, the quantizer is chosen as a Cartesian product of grids of the one-dimensional standard Gaussian random variables. So, we also immediately find the probability associated to every trajectory $\chi_{\underline{i}}^{\mathbf{d}}$: for every $\underline{i} = (i_1, \ldots, i_m) \in \prod_{n=1}^{m} \{1, \ldots, d(n)\}$,

$$\mathbb{P}(\widehat{Z}^{\mathbf{d}} = \chi_{\underline{i}}^{\mathbf{d}}) = \prod_{n=1}^{m} \mathbb{P}(\xi_n \in C_{i_n}(\Gamma^{d(n)})),$$

where $C_j(\Gamma^{d(n)})$ is the jth Voronoi cell relative to the $d(n)$-quantizer $\Gamma^{d(n)}$ in definition 3.1.

The following, proved in appendix A.1, deals with the quantization error estimation and its minimization and provides hints to choose $(m, \mathbf{d})$. A similar result on the error can be obtained applying (Luschgy and Pagès 2007, theorem 2) to the first example provided in the reference. For completeness we preferred to prove the result in an autonomous way to further characterize the explicit expression of the rate optimal parameters. Indeed, we then compare these rate optimal parameters with the (numerically computed) optimal ones in section 5.1. The symbol $\lfloor \cdot \rfloor$ denotes the lower integer part.

PROPOSITION 3.6 *Under assumption* 2.3, *for any $N \geq 1$, there exist $m^*(N) \in \mathbb{N}$ and $C > 0$ such that*

$$\mathbb{E}\left[\left\| \widehat{Z}_N^{\mathbf{d}_N^*} - Z \right\|_{L^2[0,1]}^2 \right]^{\frac{1}{2}} \leq C \log(N)^{-H},$$

where $\mathbf{d}_N^* \in \mathcal{D}_{m^*(N)}^N$ and with, for each $n = 1, \ldots, m^*(N)$,

$$d_N^*(n) = \left\lfloor N^{\frac{1}{m^*(N)}} n^{-(H+\frac{1}{2})} \left(m^*(N)! \right)^{\frac{2H+1}{2m^*(N)}} \right\rfloor.$$

Furthermore $m^*(N) = \mathcal{O}(\log(N))$.

REMARK 3.7 In the RL case, the trajectories of $\widehat{Z}^{H,\mathbf{d}}$ are easily computable and they are used in the numerical implementations to approximate the process Z^H. In practice, the parameters m and $\mathbf{d} = (d(1), \ldots, d(m))$ are chosen as explained in section 5.1.

3.1. Stationarity

We now show that the quantizers we are using are stationary. The use of stationary quantizers is motivated by the fact that their expectation provides a lower bound for the expectation of convex functionals of the process (remark 3.9) and they yield a lower (weak) error in cubature formulae (Pagès 2007, page 26). We first recall the definition of stationarity for the quadratic quantizer of a random vector (Pagès 2007, definition 1).

DEFINITION 3.8 Let X be an $\mathbb{R}^d$-valued random vector on $(\Omega, \mathcal{F}, \mathbb{P})$. A quantizer Γ for X is *stationary* if the nearest neighbor projection $\widehat{X}^{\Gamma} = \mathrm{Proj}_{\Gamma}(X)$ satisfies

$$\mathbb{E}[X|\widehat{X}^{\Gamma}] = \widehat{X}^{\Gamma}. \tag{10}$$

REMARK 3.9 Taking expectation on both sides of (10) yields $\mathbb{E}[X] = \mathbb{E}[\mathbb{E}[X|\widehat{X}^{\Gamma}]] = \mathbb{E}[\widehat{X}^{\Gamma}]$. Furthermore, for any convex

function $f : \mathbb{R}^d \to \mathbb{R}$, the identity above, the conditional Jensen's inequality and the tower property yield

$$\mathbb{E}[f(\widehat{X}^{\Gamma})] = \mathbb{E}[f(\mathbb{E}[X|\widehat{X}^{\Gamma}])] \leq \mathbb{E}[\mathbb{E}[f(X)|\widehat{X}^{\Gamma}]] = \mathbb{E}[f(X)].$$

While an optimal quadratic quantizer of order N of a random vector is always stationary (Pagès 2007, proposition 1(c)), the converse is not true in general. We now present the corresponding definition for a stochastic process.

DEFINITION 3.10 Let $\{X_t\}_{t \in [T_1, T_2]}$ be a stochastic process on $(\Omega, \mathcal{F}, \{\mathcal{F}_t\}_{t \in [T_1, T_2]}, \mathbb{P})$. We say that an N-quantizer $\Lambda^N := \{\lambda_1^N, \ldots, \lambda_N^N\} \subset L^2[T_1, T_2]$, inducing the quantization $\widehat{X} = \widehat{X}^{\Lambda^N}$, is *stationary* if $\mathbb{E}[X_t|\widehat{X}_t] = \widehat{X}_t$, for all $t \in [T_1, T_2]$.

REMARK 3.11 To ease the notation, we omit the grid Λ^N in $\widehat{X}^{\Lambda^N}$, while the dependence on the dimension N remains via the superscript $\mathbf{d} \in \mathcal{D}_m^N$ (recall (9)).

As was stated in section 2.1, we are working with the continuous version of the Gaussian Volterra process Z given by the series expansion (5). This will ease the proof of stationarity below (for a similar result in the case of the Brownian motion (Pagès 2007, proposition 2)).

PROPOSITION 3.12 *The product functional quantizers inducing $\widehat{Z}^{\mathbf{d}}$ in (9) are stationary.*

Proof For any $t \in [0, 1]$, by linearity, we have the following chain of equalities:

$$\mathbb{E}\left[Z_t | \{\widehat{\xi}_n^{d(n)}\}_{1 \leq n \leq m} \right] = \mathbb{E}\left[\sum_{k \geq 1} \mathcal{K}[\psi_k](t) \xi_k \Big| \{\widehat{\xi}_n^{d(n)}\}_{1 \leq n \leq m} \right]$$
$$= \sum_{k \geq 1} \mathcal{K}[\psi_k](t) \mathbb{E}\left[\xi_k \Big| \{\widehat{\xi}_n^{d(n)}\}_{1 \leq n \leq m} \right].$$

Since the $\mathcal{N}(0, 1)$-Gaussian ξ_n's are i.i.d., by definition of optimal quadratic quantizers (hence stationary), we have $\mathbb{E}[\xi_k|\widehat{\xi}_i^{d(i)}] = \delta_{ik}\widehat{\xi}_i^{d(i)}$, for all $i, k \in \{1, \ldots, m\}$, and therefore

$$\mathbb{E}\left[\xi_k \Big| \{\widehat{\xi}_n^{d(n)}\}_{1 \leq n \leq m} \right] = \mathbb{E}\left[\xi_k \Big| \widehat{\xi}_k^{d(k)} \right] = \widehat{\xi}_k^{d(k)},$$
$$\text{for all } k \in \{1, \ldots, m\}.$$

Thus we obtain

$$\mathbb{E}\left[Z_t \Big| \{\widehat{\xi}_n^{d(n)}\}_{1 \leq n \leq m} \right] = \sum_{k \geq 1} \mathcal{K}[\psi_k](t) \widehat{\xi}_k^{d(k)} = \widehat{Z}_t^{\mathbf{d}}.$$

Finally, exploiting the tower property and the fact that the σ-algebra generated by $\widehat{Z}_t^{\mathbf{d}}$ is included in the σ-algebra generated by $\{\widehat{\xi}_n^{d(n)}\}_{n \in \{1, \ldots, m\}}$ by definition 3.2, we obtain

$$\mathbb{E}\left[Z_t \Big| \widehat{Z}_t^{\mathbf{d}} \right] = \mathbb{E}\left[\mathbb{E}\left[Z_t \Big| \{\widehat{\xi}_n^{d(n)}\}_{n \in \{1, \ldots, m\}} \right] \Big| \widehat{Z}_t^{\mathbf{d}} \right] = \mathbb{E}\left[\widehat{Z}_t^{\mathbf{d}} \Big| \widehat{Z}_t^{\mathbf{d}} \right]$$
$$= \widehat{Z}_t^{\mathbf{d}},$$

which concludes the proof. ∎

4. Application to VIX derivatives in rough Bergomi

We now specialize the setup above to the case of rough volatility models. These models are extensions of classical stochastic volatility models, introduced to better reproduce the market implied volatility surface. The volatility process is stochastic and driven by a rough process, by which we mean a process whose trajectories are H-Hölder continuous with $H \in (0, \frac{1}{2})$. The empirical study (Gatheral *et al.* 2018) was the first to suggest such a rough behavior for the volatility, and ignited tremendous interest in the topic. The website https://sites.google.com/site/roughvol/home contains an exhaustive and up-to-date review of the literature on rough volatility. Unlike continuous Markovian stochastic volatility models, which are not able to fully describe the steep implied volatility skew of short-maturity options in equity markets, rough volatility models have shown accurate fit for this crucial feature. Within rough volatility, the rough Bergomi model (Bayer *et al.* 2016) is one of the simplest, yet decisive frameworks to harness the power of the roughness for pricing purposes. We show how to adapt our functional quantization setup to this case.

4.1. The generalized Bergomi model

We work here with a slightly generalized version of the rough Bergomi model, defined as

$$
\begin{cases}
X_t = -\dfrac{1}{2} \displaystyle\int_0^t \mathcal{V}_s \, ds + \int_0^t \sqrt{\mathcal{V}_s} \, dB_s, & X_0 = 0, \\
\mathcal{V}_t = v_0(t) \exp\left\{ \gamma Z_t - \dfrac{\gamma^2}{2} \displaystyle\int_0^t K(t-s)^2 \, ds \right\}, & \mathcal{V}_0 > 0,
\end{cases}
$$

where X is the log-stock price, $\mathcal{V}$ the instantaneous variance process driven by the Gaussian Volterra process Z in (1), $\gamma > 0$ and B is a Brownian motion defined as $B := \rho W + \sqrt{1 - \rho^2} W^\perp$ for some correlation $\rho \in [-1, 1]$ and $W, W^\perp$ orthogonal Brownian motions. The filtered probability space is therefore taken as $\mathcal{F}_t = \mathcal{F}_t^W \vee \mathcal{F}_t^{W^\perp}$, $t \geq 0$. This is a non-Markovian generalization of Bergomi's second generation stochastic volatility model (Bergomi 2005), letting the variance be driven by a Gaussian Volterra process instead of a standard Brownian motion. Here, $v_T(t)$ denotes the forward variance for a remaining maturity t, observed at time T. In particular, v_0 is the initial forward variance curve, assumed to be $\mathcal{F}_0$-measurable. Indeed, given market prices of variance swaps $\sigma_T^2(t)$ at time T with remaining maturity t, the forward variance curve can be recovered as $v_T(t) = \frac{d}{dt}(t\sigma_T^2(t))$, for all $t \geq 0$, and the process $\{v_s(t-s)\}_{0 \leq s \leq t}$ is a martingale for all fixed $t > 0$.

REMARK 4.1 With $K(u) = u^{H-\frac{1}{2}}$, $\gamma = 2\nu C_H$, for $\nu > 0$, and $C_H := \sqrt{\frac{2H\Gamma(3/2-H)}{\Gamma(H+1/2)\Gamma(2-2H)}}$, we recover the standard rough Bergomi model (Bayer *et al.* 2016).

4.2. VIX Futures in the generalized Bergomi

We consider the pricing of VIX Futures (www.cboe.com/tradable_products/vix/) in the rough Bergomi model. They are highly liquid Futures on the Chicago Board Options Exchange Volatility Index, introduced on March 26, 2004, to allow for trading in the underlying VIX. Each VIX Future represents the expected implied volatility for the 30 days following the expiration date of the Futures contract itself. The continuous version of the VIX at time T is determined by the continuous-time monitoring formula

$$
\begin{aligned}
\mathrm{VIX}_T^2 &:= \mathbb{E}_T\left[\frac{1}{\Delta} \int_T^{T+\Delta} d\langle X_s, X_s \rangle \right] = \frac{1}{\Delta} \int_T^{T+\Delta} \mathbb{E}[\mathcal{V}_s | \mathcal{F}_T] \, ds \\
&= \frac{1}{\Delta} \int_T^{T+\Delta} \mathbb{E}_T\left[v_0(s) e^{\gamma Z_s - \frac{\gamma^2}{2} \int_0^s K(s-u)^2 \, du} \right] ds \\
&= \frac{1}{\Delta} \int_T^{T+\Delta} v_0(s) e^{\gamma \int_0^T K(s-u) \, dW_u - \frac{\gamma^2}{2} \int_0^s K(s-u)^2 \, du} \\
&\quad \times \mathbb{E}_T\left[e^{\gamma \int_T^s K(s-u) \, dW_u} \right] ds \\
&= \frac{1}{\Delta} \int_T^{T+\Delta} v_0(s) e^{\gamma \int_0^T K(s-u) \, dW_u - \frac{\gamma^2}{2} \int_0^s K(s-u)^2 \, du} \\
&\quad \times e^{\frac{\gamma^2}{2} \int_T^s K(s-u)^2 \, du} \, ds, \tag{11}
\end{aligned}
$$

similarly to Jacquier *et al.* (2018a), where Δ is equal to 30 days, and we write $\mathbb{E}_T[\cdot] := \mathbb{E}[\cdot|\mathcal{F}_T]$ (dropping the subscript when $T = 0$). Thus the price of a VIX Future with maturity T is given by

$$
\begin{aligned}
\mathcal{P}_T &:= \mathbb{E}[\mathrm{VIX}_T] \\
&= \mathbb{E}\Bigg[\bigg(\frac{1}{\Delta} \int_T^{T+\Delta} v_0(t) \\
&\quad \times e^{\gamma Z_t^{T,\Delta} + \frac{\gamma^2}{2} \left(\int_0^{t-T} K(s)^2 \, ds - \int_0^t K(s)^2 \, ds \right)} \, dt \bigg)^{\frac{1}{2}} \Bigg],
\end{aligned}
$$

where the process $(Z_t^{T,\Delta})_{t \in [T, T+\Delta]}$ is given by

$$
Z_t^{T,\Delta} = \int_0^T K(t-s) \, dW_s, \quad t \in [T, T+\Delta].
$$

To develop a functional quantization setup for VIX Futures, we need to quantize the process $Z^{T,\Delta}$, which is close, yet slightly different, from the Gaussian Volterra process Z in (1).

4.3. Properties of Z^T

To retrieve the same setting as above, we normalize the time interval to $[0, 1]$, that is $T + \Delta = 1$. Then, for T fixed, we define the process $Z^T := Z^{T, 1-T}$ as

$$
Z_t^T := \int_0^T K(t-s) \, dW_s, \quad t \in [T, 1],
$$

which is well defined by the square integrability of K. By definition, the process Z^T is centered Gaussian and Itô isometry gives its covariance function as

$$
R_{Z^T}(t, s) = \int_0^T K(t-u)K(s-u) \, du, \quad t, s \in [T, 1].
$$

Proceeding as previously, we introduce a Gaussian process with same mean and covariance as those of Z^T, represented as

a series expansion involving standard Gaussian variables; from which product functional quantization follows. It is easy to see that the process Z^T has continuous trajectories. Indeed, $(Z_t^T - Z_s^T)^2 \leq \mathbb{E}[|Z_t - Z_s|^2 | \mathcal{F}_T^W]$, by conditional Jensen's inequality since $Z_t^T = \mathbb{E}[Z_t | \mathcal{F}_T^W]$. Then, applying tower property, for any $T \leq s < t \leq 1$,

$$\mathbb{E}\left[\left|Z_t^T - Z_s^T\right|^2\right] \leq \mathbb{E}\left[|Z_t - Z_s|^2\right],$$

and therefore the H-Hölder regularity of Z (section 2) implies that of Z^T.

4.3.1. Series expansion. Let $\{\xi_n\}_{n \geq 1}$ be an i.i.d. sequence of standard Gaussian and $\{\psi_n\}_{n \geq 1}$ the orthonormal basis of $L^2[0, 1]$ from (3). Denote by $\mathcal{K}^T(\cdot)$ the operator from $L^2[0, 1]$ to $\mathcal{C}[T, 1]$ that associates to each $f \in L^2[0, 1]$,

$$\mathcal{K}^T[f](t) := \int_0^T K(t - s)f(s)\, \mathrm{d}s, \quad t \in [T, 1]. \quad (12)$$

We define the process Y^T as (recall the analogous (2)):

$$Y_t^T := \sum_{n \geq 1} \mathcal{K}^T[\psi_n](t)\xi_n, \quad t \in [T, 1].$$

The lemma below follows from the corresponding results in remark 2.2 and lemma 2.4:

LEMMA 4.2 *The process Y^T is centered, Gaussian and with covariance function*

$$R_{Y^T}(s, t) := \mathbb{E}\left[Y_s^T Y_t^T\right]$$
$$= \int_0^T K(t - u)K(s - u)\, \mathrm{d}u, \quad \text{for all } s, t \in [T, 1].$$

To complete the analysis of Z^T, we require an analogue version of assumption 2.3.

ASSUMPTION 4.3 Assumption 2.3 holds for the sequence $(\mathcal{K}^T[\psi_n])_{n \geq 1}$ on $[T, 1]$ with the constants C_1 and C_2 depending on T.

4.4. The truncated RL case

We again pay special attention to the RL case, for which the operator (12) reads, for each $n \in \mathbb{N}$,

$$\mathcal{K}_H^T[\psi_n](t) := \int_0^T (t - s)^{H - \frac{1}{2}} \psi_n(s)\, \mathrm{d}s, \quad \text{for all } t \in [T, 1],$$

and satisfies the following, proved in appendix A.4.

LEMMA 4.4 *The functions $\{\mathcal{K}_H^T[\psi_n]\}_{n \geq 1}$ satisfy assumption 4.3.*

A key role in this proof is played by an intermediate lemma, proved in appendix A.3, which provides a convenient representation for the integral $\int_0^T (t - u)^{H - \frac{1}{2}} \mathrm{e}^{\mathrm{i}\pi u} du$, $t \geq T \geq 0$, in terms of the generalized Hypergeometric function $_1F_2(\cdot)$.

LEMMA 4.5 *For any $t \geq T \geq 0$, the representation*

$$\int_0^T (t - u)^{H - \frac{1}{2}} \mathrm{e}^{\mathrm{i}\pi u}\, \mathrm{d}u = \mathrm{e}^{\mathrm{i}\pi t} \left[\left(\zeta_{\frac{1}{2}}(t, h_1) - \zeta_{\frac{1}{2}}((t - T), h_1)\right)\right.$$
$$\left. - \mathrm{i}\pi \left(\zeta_{\frac{3}{2}}(t, h_2) - \zeta_{\frac{3}{2}}((t - T), h_2)\right)\right]$$

holds, where $h_1 := \frac{1}{2}(H + \frac{1}{2})$ and $h_2 = \frac{1}{2} + h_1$, $\chi(z) := -\frac{1}{4}\pi^2 z^2$ and

$$\zeta_k(z, h) := \frac{z^{2h}}{2h} {}_1F_2(h; k, 1 + h; \chi(z)), \quad \text{for } k \in \left\{\frac{1}{2}, \frac{3}{2}\right\}. \quad (13)$$

REMARK 4.6 The representation in lemma 4.5 can be exploited to obtain an explicit formula for $\mathcal{K}_H^T[\psi_n](t)$, $t \in [T, 1]$ and $n \in \mathbb{N}$:

$$\mathcal{K}_H^T[\psi_n](t)$$
$$= \frac{\sqrt{2}}{m^{H + \frac{1}{2}}} \int_0^{mT} (mt - u)^{H - \frac{1}{2}} \cos(\pi u)\, \mathrm{d}u$$
$$= \frac{\sqrt{2}}{m^{H + \frac{1}{2}}} \Re\left\{\int_0^{mT} (mt - u)^{H - \frac{1}{2}} \mathrm{e}^{\mathrm{i}\pi u}\, \mathrm{d}u\right\}$$
$$= \frac{\sqrt{2}}{m^{H + \frac{1}{2}}} \Re\left\{\mathrm{e}^{\mathrm{i}\pi mt} \left[\left(\zeta_{\frac{1}{2}}(mt, h_1) - \zeta_{\frac{1}{2}}(m(t - T), h_1)\right)\right.\right.$$
$$\left.\left. - \mathrm{i}\pi \left(\zeta_{\frac{3}{2}}(mt, h_2) - \zeta_{\frac{3}{2}}(m(t - T), h_2)\right)\right]\right\}$$
$$= \frac{\sqrt{2}}{m^{H + \frac{1}{2}}} \left\{\cos(mt\pi) \left(\zeta_{\frac{1}{2}}(mt, h_1) - \zeta_{\frac{1}{2}}(m(t - T), h_1)\right)\right.$$
$$\left. + \pi \sin(mt\pi) \left(\zeta_{\frac{3}{2}}(mt, h_2) - \zeta_{\frac{3}{2}}(m(t - T), h_2)\right)\right\},$$

with $m := n - \frac{1}{2}$ and $\zeta_{\frac{1}{2}}(\cdot)$, $\zeta_{\frac{3}{2}}(\cdot)$ in (13). We shall exploit this in our numerical simulations.

4.5. VIX derivatives pricing

We can now introduce the quantization for the process $Z^{T, \Delta}$, similarly to definition 3.2, recalling the definition of the set $\mathcal{D}_m^N$ in (8):

DEFINITION 4.7 *A product functional quantization for $Z^{T, \Delta}$ of order N is defined as*

$$\widehat{Z}_t^{T, \Delta, \mathbf{d}} := \sum_{n=1}^m \mathcal{K}^{T, \Delta}[\psi_n^{T, \Delta}](t)\widehat{\xi}_n^{d(n)}, \quad t \in [T, T + \Delta],$$

where $\mathbf{d} \in \mathcal{D}_m^N$, for some $m \in \mathbb{N}$, and for every $n \in \{1, \ldots, m\}$, $\widehat{\xi}_n^{d(n)}$ is the (unique) optimal quadratic quantization of the Gaussian variable ξ_n of order $d(n)$.

The sequence $\{\psi_n^{T, \Delta}\}_{n \in \mathbb{N}}$ denotes the orthonormal basis of $L^2[0, T + \Delta]$ given by

$$\psi_n^{T, \Delta}(t) = \sqrt{\frac{2}{T + \Delta}} \cos\left(\frac{t}{\sqrt{\lambda_n}(T + \Delta)}\right), \quad \text{with}$$
$$\lambda_n = \frac{4}{(2n - 1)^2 \pi^2},$$

and the operator $\mathcal{K}^{T,\Delta} : L^2[0, T + \Delta] \to \mathcal{C}[T, T + \Delta]$ is defined for $f \in L^2[0, T + \Delta]$ as

$$\mathcal{K}^{T,\Delta}[f](t) := \int_0^T K(t - s) f(s) \, ds, \quad t \in [T, T + \Delta].$$

Adapting the proof of proposition 3.12, it is possible to prove that these quantizers are stationary, too.

REMARK 4.8 The dependence on Δ is due to the fact that the coefficients in the series expansion depend on the time interval $[T, T + \Delta]$.

In the RL case for each $n \in \mathbb{N}$, we can write, using remark 4.6, for any $t \in [T, T + \Delta]$:

$$\mathcal{K}_H^{T,\Delta}[\psi_n^{T,\Delta}](t)$$

$$= \sqrt{\frac{2}{T + \Delta}} \int_0^T (t - s)^{H - \frac{1}{2}} \cos\left(\frac{s}{\sqrt{\lambda_n}(T + \Delta)}\right) ds,$$

$$= \frac{\sqrt{2}(T + \Delta)^H}{(n - 1/2)^{H + \frac{1}{2}}} \int_0^{\frac{(n - 1/2)}{T + \Delta} T} \left(\frac{(n - 1/2)}{T + \Delta} t - u\right)^{H - \frac{1}{2}} \cos(\pi u) \, du$$

$$= \frac{\sqrt{2}(T + \Delta)^H}{(n - \frac{1}{2})^{H + \frac{1}{2}}} \left\{ \cos\left(\frac{(n - \frac{1}{2})}{T + \Delta} t \pi\right) \left(\zeta_{\frac{1}{2}}\left(\frac{(n - \frac{1}{2})}{T + \Delta} t, h_1\right) \right. \right.$$

$$+ \left. -\zeta_{\frac{1}{2}}\left(\frac{(n - \frac{1}{2})}{T + \Delta}(t - T), h_1\right)\right)$$

$$+ \pi \sin\left(\frac{(n - \frac{1}{2})}{T + \Delta} t \pi\right) \left(\zeta_{\frac{3}{2}}\left(\frac{(n - \frac{1}{2})}{T + \Delta} t, h_2\right) \right.$$

$$+ \left. \left. -\zeta_{\frac{3}{2}}\left(\frac{(n - \frac{1}{2})}{T + \Delta}(t - T), h_2\right)\right)\right\}.$$

We thus exploit $\widehat{Z}^{T,\Delta,\mathbf{d}}$ to obtain an estimation of VIX_T and of VIX Futures through the following:

$$\widehat{\text{VIX}}_T^{\mathbf{d}} := \left(\frac{1}{\Delta} \int_T^{T+\Delta} v_0(t) \exp\left\{\gamma \widehat{Z}_t^{T,\Delta,\mathbf{d}} + \frac{\gamma^2}{2}\right.\right.$$

$$\times \left. \left. \left(\int_0^{t-T} K(s)^2 \, ds - \int_0^t K(s)^2 \, ds\right)\right\} dt\right)^{\frac{1}{2}},$$

$$\widehat{\mathcal{P}}_T^{\mathbf{d}} := \mathbb{E}\left[\left(\frac{1}{\Delta} \int_T^{T+\Delta} v_0(t) \exp\left\{\gamma \widehat{Z}_t^{T,\Delta,\mathbf{d}} + \frac{\gamma^2}{2}\right.\right.\right.$$

$$\times \left. \left. \left. \left(\int_0^{t-T} K(s)^2 \, ds - \int_0^t K(s)^2 \, ds\right)\right\} dt\right)^{\frac{1}{2}}\right].$$
(14)

REMARK 4.9 The expectation above reduces to the following deterministic summation, making its computation immediate:

$$\widehat{\mathcal{P}}_T^{\mathbf{d}} = \mathbb{E}\left[\left(\frac{1}{\Delta} \int_T^{T+\Delta} v_0(t)\right.\right.$$

$$e^{\gamma \sum_{n=1}^m \mathcal{K}^{T,\Delta}[\psi_n^{T,\Delta}](t)\widehat{\xi}_n^{d(n)} + \frac{\gamma^2}{2}\left(\int_0^{t-T} K(s)^2 \, ds - \int_0^t K(s)^2 \, ds\right)} dt\right)^{\frac{1}{2}}\right]$$

$$= \sum_{\underline{i} \in I^d} \left(\frac{1}{\Delta} \int_T^{T+\Delta} v_0(t)\right.$$

$$e^{\gamma \sum_{n=1}^m \mathcal{K}^{T,\Delta}[\psi_n^{T,\Delta}](t) x_{i_n}^{d(n)} + \frac{\gamma^2}{2}\left(\int_0^{t-T} K(s)^2 \, ds - \int_0^t K(s)^2 \, ds\right)} dt\right)^{\frac{1}{2}}$$

$$\cdot \prod_{n=1}^m \mathbb{P}(\xi_n \in C_{i_n}(\Gamma^{d(n)})),$$

where $\widehat{\xi}_n^{d(n)}$ is the (unique) optimal quadratic quantization of ξ_n of order $d(n)$, $C_j(\Gamma^{d(n)})$ is the jth Voronoi cell relative to the $d(n)$-quantizer (definition 3.1), with $j = 1, \ldots, d(n)$ and $\underline{i} = (i_1, \ldots, i_m) \in \prod_{j=1}^m \{1, \ldots, d(j)\}$. In the numerical illustrations displayed in section 5, we exploited Simpson rule to evaluate these integrals. In particular, we used *simps* function from *scipy.integrate* with 300 points.

4.6. Quantization error of VIX derivatives

The following L^2-error estimate is a consequence of assumption 4.3 (B) and its proof is omitted since it is analogous to that of proposition 3.6:

PROPOSITION 4.10 *Under assumption 4.3, for any $N \geq 1$, there exist $m_T^*(N) \in \mathbb{N}$, $C > 0$ such that*

$$\mathbb{E}\left[\left\|\widehat{Z}^{T,\Delta,\mathbf{d}_{T,N}^*} - Z^{T,\Delta}\right\|_{L^2[T,T+\Delta]}^2\right]^{\frac{1}{2}} \leq C \log(N)^{-H},$$

for $\mathbf{d}_{T,N}^* \in \mathcal{D}_{m_T^*(N)}^N$ and with, for each $n = 1, \ldots, m_T^*(N)$,

$$d_{T,N}^*(n) = \left\lfloor N^{\frac{1}{m_T^*(N)}} n^{-(H + \frac{1}{2})} \left(m_T^*(N)!\right)^{\frac{2H+1}{2m_T^*(N)}}\right\rfloor.$$

Furthermore $m_T^*(N) = \mathcal{O}(\log(N))$.

As a consequence, we have the following error quantification for European options on the VIX:

THEOREM 4.11 *Let $F : \mathbb{R} \to \mathbb{R}$ be a globally Lipschitz-continuous function and $\mathbf{d} \in \mathbb{N}^m$ for some $m \in \mathbb{N}$. There exists $\mathfrak{K} > 0$ such that*

$$\left|\mathbb{E}[F(\text{VIX}_T)] - \mathbb{E}\left[F\left(\widehat{\text{VIX}}_T^{\mathbf{d}}\right)\right]\right|$$

$$\leq \mathfrak{K}\,\mathbb{E}\left[\left\|Z^{T,\Delta} - \widehat{Z}^{T,\Delta,\mathbf{d}}\right\|_{L^2([T,T+\Delta])}^2\right]^{\frac{1}{2}}. \quad (15)$$

Furthermore, for any $N \geq 1$, there exist $m_T^*(N) \in \mathbb{N}$ and $\mathfrak{C} > 0$ such that, with $\mathbf{d}_{T,N}^* \in \mathcal{D}_{m_T^*(N)}^N$,

$$\left|\mathbb{E}[F(\text{VIX}_T)] - \mathbb{E}\left[F\left(\widehat{\text{VIX}}_T^{\mathbf{d}_{T,N}^*}\right)\right]\right| \leq \mathfrak{C} \log(N)^{-H}. \quad (16)$$

The upper bound in (16) is an immediate consequence of (15) and proposition 4.10. The proof of (15) is much more involved and is postponed to appendix A.5.

REMARK 4.12 • When $F(x) = 1$, we obtain the price of VIX Futures and the quantization error

$$\left|\mathcal{P}_T - \widehat{\mathcal{P}}_T^{\mathbf{d}}\right| \leq \mathfrak{K}\,\mathbb{E}\left[\left\|Z^{T,\Delta} - \widehat{Z}^{T,\Delta,\mathbf{d}}\right\|_{L^2([T,T+\Delta])}^2\right]^{\frac{1}{2}},$$

and, for any $N \geq 1$, theorem 4.11 yields the existence of $m_T^*(N) \in \mathbb{N}$, $\mathfrak{C} > 0$ such that

$$\left|\mathcal{P}_T - \widehat{\mathcal{P}}_T^{\mathbf{d}_{T,N}^*}\right| \leq \mathfrak{C} \log(N)^{-H}.$$

- Since the functions $F(x) := (x - K)_+$ and $F(x) := (K - x)_+$ are globally Lipschitz continuous, the same bounds apply for European Call and Put options on the VIX.

5. Numerical results for the RL case

We now test the quality of the quantization on the pricing of VIX Futures in the standard rough Bergomi model, considering the RL kernel in remark 4.1.

5.1. Practical considerations for m and **d**

Proposition 3.6 provides, for any fixed $N \in \mathbb{N}$, some indications on $m^*(N)$ and $\mathbf{d}_N^* \in \mathcal{D}_m^N$ (see (8)), for which the rate of convergence of the quantization error is $\log(N)^{-H}$. We present now a numerical algorithm to compute the optimal parameters. For a given number of trajectories $N \in \mathbb{N}$, the problem is equivalent to finding $m \in \mathbb{N}$ and $\mathbf{d} \in \mathcal{D}_m^N$ such that $\mathbb{E}[\|Z^H - \widehat{Z}^{H,\mathbf{d}}\|_{L^2[0,1]}^2]$ is minimal. Starting from (A1) and adding and subtracting the quantity $\sum_{n=1}^m (\int_0^1 \mathcal{K}_H[\psi_n](t)^2 \, dt)$, we obtain

$$\mathbb{E}\left[\left\|Z^H - \widehat{Z}^{H,\mathbf{d}}\right\|_{L^2[0,1]}^2\right]$$

$$= \sum_{n=1}^m \left(\int_0^1 \mathcal{K}_H[\psi_n](t)^2 \, dt\right)$$

$$[\boldsymbol{\varepsilon}^{d(n)}(\xi_n)]^2 + \sum_{k \geq m+1} \int_0^1 \mathcal{K}_H[\psi_k](t)^2 \, dt$$

$$= \sum_{n=1}^m \left(\int_0^1 \mathcal{K}_H[\psi_n](t)^2 \, dt\right)$$

$$s\left\{[\boldsymbol{\varepsilon}^{d(n)}(\xi_n)]^2 - 1\right\} + \sum_{k \geq 1} \int_0^1 \mathcal{K}_H[\psi_k](t)^2 \, dt, ix \quad (17)$$

where $\boldsymbol{\varepsilon}^{d(n)}(\xi_n)$ denotes the optimal quadratic quantization error for the quadratic quantizer of order $d(n)$ of the standard Gaussian random variable ξ_n (see appendix A.1 for more details). Note that the last term on the right-hand side of (17) does not depend on m, nor on $\mathbf{d}$. We therefore simply look for m and $\mathbf{d}$ that minimize

$$A(m, \mathbf{d}) := \sum_{n=1}^m \left(\int_0^1 \mathcal{K}_H[\psi_n]^2(t) \, dt\right) \left([\boldsymbol{\varepsilon}^{d(n)}(\xi_n)]^2 - 1\right).$$

This can be easily implemented: the functions $\mathcal{K}_H[\psi_n]$ can be obtained numerically from the Hypergeometric function and the quadratic errors $\boldsymbol{\varepsilon}^{d(n)}(\xi_n)$ are available at www.quantize.maths-fi.com/gaussian_database, for $d(n) \in \{1, \ldots, 5999\}$. The algorithm therefore reads as follows:

(i) fix m;
(ii) minimize $A(m, \mathbf{d})$ over $\mathbf{d} \in \mathcal{D}_m^N$ and call it $\widetilde{A}(m)$;
(iii) minimize $\widetilde{A}(m)$ over $m \in \mathbb{N}$.

The results of the algorithm for some reference values of $N \in \mathbb{N}$ are available in table 1, where $\overline{N}_{traj} := \prod_{i=1}^{\overline{m}(N)} \overline{d}_N(i)$

Table 1. Optimal parameters.

N	$\overline{m}(N)$	$\overline{\mathbf{d}}_N$	$\overline{N}_{traj}$
10	2	5 - 2	10
10^2	4	8 - 3 - 2 - 2	96
10^3	6	10 - 4 - 3 - 2 - 2 - 2	960
10^4	8	10 - 5 - 4 - 3 - 2 - 2 - 2 - 2	9600
10^5	10	14 - 6 - 4 - 3 - 3 - 2 - 2 - 2 - 2 - 2	96768
10^6	12	14 - 6 - 5 - 4 - 3 - 3 - 2 - 2 - 2 - 2 - 2 - 2	967680

represents the number of trajectories actually computed in the optimal case. In table 2, we compute the rate optimal parameters derived in proposition 3.6: the column 'Relative error' contains the normalized difference between the L^2-quantization error made with the optimal choice of $\overline{m}(N)$ and $\overline{\mathbf{d}}_N$ in table 1 and the L^2-quantization error made with $m^*(N)$ and $\mathbf{d}_N^*$ of the corresponding line of the table, namely $\frac{|\|Z^H - \widehat{Z}^{H,\overline{\mathbf{d}}_N}\|_{L^2[0,1]} - \|Z^H - \widehat{Z}^{H,\mathbf{d}_N^*}\|_{L^2[0,1]}|}{\|Z^H - \widehat{Z}^{H,\overline{\mathbf{d}}_N}\|_{L^2[0,1]}}$. In the column $N_{traj}^* := \prod_{i=1}^{m^*(N)} d_N^*(i)$ we display the number of trajectories actually computed in the rate-optimal case. The optimal quadratic vector quantization of a standard Gaussian of order 1 is the random variable identically equal to zero and so when $d(i) = 1$ the corresponding term is uninfluential in the representation.

5.2. The functional quantizers

The computations in sections 2 and 3 for the RL process, respectively the ones in sections 4.3 and 4.4 for $Z^{H,T}$, provide a way to obtain the functional quantizers of the processes.

5.2.1. Quantizers of the RL process. For the RL process, definition 3.4 shows that its quantizer is a weighted Cartesian product of grids of the one-dimensional standard Gaussian random variables. The time-dependent weights $\mathcal{K}_H[\psi_n](\cdot)$ are computed using (7), and for a fixed number of trajectories N, suitable $\overline{m}(N)$ and $\overline{\mathbf{d}}_N \in \mathcal{D}_{\overline{m}(N)}^N$ are chosen according to the algorithm in section 5.1. Not surprisingly, figure 1 shows that as the paths of the process get smoother (H increases) the trajectories become less fluctuating and shrink around zero. For $H = 0.5$, where the RL process reduces to the standard Brownian motion, we recover the well-known quantizer from Pagès (2007, figures 7–8). This is consistent as in that case $\mathcal{K}_H[\psi_n](t) = \sqrt{\lambda_n}\sqrt{2}\sin(\frac{t}{\sqrt{\lambda_n}})$, and so Y^H is the Karhuenen–Loève expansion for the Brownian motion (Pagès 2007, section 7.1).

5.2.2. Quantizers of $Z^{H,T}$. A quantizer for $Z^{H,T}$ is defined analogously to that of Z^H using Definition 3.4. The weights $\mathcal{K}_H^T[\psi_n](\cdot)$ in the summation are available in closed form, as shown in Remark 4.6. It is therefore possible to compute the N-product functional quantizer, for any $N \in \mathbb{N}$, as figure 2 displays.

5.3. Pricing and comparison with Monte Carlo

In this section, we show and comment some plots related to the estimation of prices of derivatives on the VIX and realized

Table 2. Rate-optimal parameters.

N	$m^*(N) = \lfloor \log(N) \rfloor$	Relative error	$\mathbf{d}_N^*$	N_{traj}^*
10	2	2.75%	3 - 2	6
10^2	4	1.30%	5 - 3 - 2 - 2	60
10^3	6	1.09%	6 - 4 - 3 - 2 - 2 - 2	576
10^4	9	3.08%	6 - 4 - 3 - 2 - 2 - 2 - 2 - 1 - 1	1152
10^5	11	3.65%	7 - 4 - 3 - 3 - 2 - 2 - 2 - 2 - 1 - 1 - 1	4032
10^6	13	2.80%	8 - 5 - 4 - 3 - 3 - 2 - 2 - 2 - 2 - 1 - 1 - 1	46080
N	$m^*(N) = \lfloor \log(N) \rfloor$ - 1	Relative error	$\mathbf{d}_N^*$	N_{traj}^*
10	1	2.78%	10	10
10^2	3	1.13%	6 - 4 - 3	72
10^3	5	1.22%	7 - 4 - 3 - 3 - 2	504
10^4	8	1.35%	7 - 4 - 3 - 3 - 2 - 2 - 2 - 2	4032
10^5	10	2.29%	7 - 5 - 4 - 3 - 2 - 2 - 2 - 2 - 2 - 1	13440
10^6	12	2.25%	8 - 5 - 4 - 3 - 3 - 2 - 2 - 2 - 2 - 2 - 2 - 1	92160
N	$m^*(N) = \lfloor \log(N) \rfloor$ - 2	Relative error	$\mathbf{d}_N^*$	N_{traj}^*
10^2	2	2.53%	12 - 8	96
10^3	4	1.44%	9 - 5 - 4 - 3	540
10^4	7	1.46%	7 - 5 - 4 - 3 - 2 - 2 - 2	3360
10^5	9	1.57%	8 - 5 - 4 - 3 - 3 - 2 - 2 - 2 - 2	23040
10^6	11	1.48%	9 - 6 - 4 - 3 - 3 - 3 - 2 - 2 - 2 - 2 - 2	186624

variance. We set the values $H = 0.1$ and $\nu = 1.18778$ for the parameters and investigate three different initial forward variance curves $v_0(\cdot)$, as in Jacquier *et al.* (2018a):

Scenario 1. $v_0(t) = 0.234^2$;
Scenario 2. $v_0(t) = 0.234^2(1 + t)^2$;
Scenario 3. $v_0(t) = 0.234^2\sqrt{1 + t}$.

The choice of such ν is a consequence of the choice $\eta = 1.9$, consistently with Bennedsen *et al.* (2017), and of the relationship $\nu = \eta\frac{\sqrt{2H}}{2C_H}$. In all these cases, v_0 is an increasing function of time, whose value at zero is close to the square of the reference value of 0.25.

5.3.1. VIX Futures pricing. One of the most recent and effective way to compute the price of VIX Futures is a Monte-Carlo-simulation method based on Cholesky decomposition, for which we refer to Jacquier *et al.* (2018a, section 3.3.2). It can be considered as a good approximation of the true price when the number M of computed paths is large. In fact, in Jacquier *et al.* (2018a) the authors tested three simulation-based methods (Hybrid scheme + forward Euler, Truncated Cholesky, SVD decomposition) and 'all three methods seem to approximate the prices similarly well'. We thus consider the truncated Cholesky approach as a benchmark and take $M = 10^6$ trajectories and 300 equidistant point for the time grid.

In figure 3, we plot the VIX Futures prices as a function of the maturity T, where T ranges in {1, 2, 3, 6, 9, 12} months (consistently with actual quotations) on the left, and the corresponding relative error w.r.t. the Monte Carlo benchmark on the right. It is clear that the quantization approximates the benchmark from below and that the accuracy increases with the number of trajectories.

We highlight that the quantization scheme for VIX Futures can be sped up considerably by storing ahead the quantized

trajectories for $Z^{H,T,\Delta}$, so that we only need to compute the integrations and summations in remark 4.9, which are extremely fast.

Furthermore, the grid organization time itself is not that significant. In table 3, we display the grid organization times (in seconds) as a function of the maturity (rows) expressed in months and of the number of trajectories (columns). From this table, one might deduce that the time needed for the organization of the grids is suitable to be performed once per day (say every morning) as it should be for actual pricing purposes. It is interesting to note that the estimations obtained with quantization (which is an exact method) are consistent in that they mimic the trend of benchmark prices over time even for very small values of N. However, as a consequence of the variance in the estimations, the Monte Carlo prices are almost useless for small values of M. Moreover, improving the estimations with Monte Carlo requires to increase the number of points in the time grid with clear impact on computational time, while this is not the case with quantization since the trajectories in the quantizers are smooth. Indeed, the trajectories in the quantizers are not only smooth but also almost constant over time, hence reducing the number of time steps to get the desired level of accuracy. Note that here we may refer also to the issue of complexity related to discretization: a quadrature formula over n points has a cost $\mathcal{O}(n)$, while the simulation with a Cholesky method over the same grid has cost $\mathcal{O}(n^2)$. Finally, our quantization method does not require much RAM. Indeed, all the simulations performed with quantization can be easily run on a personal laptop,† while this is not the case for the

---

† The personal computer used to run the quantization codes has the following technical specifications: RAM: 8.00 GB, SSD memory: 512 GB, Processor: AMD Ryzen 7 4700U with Radeon Graphics 2.00 GHz.
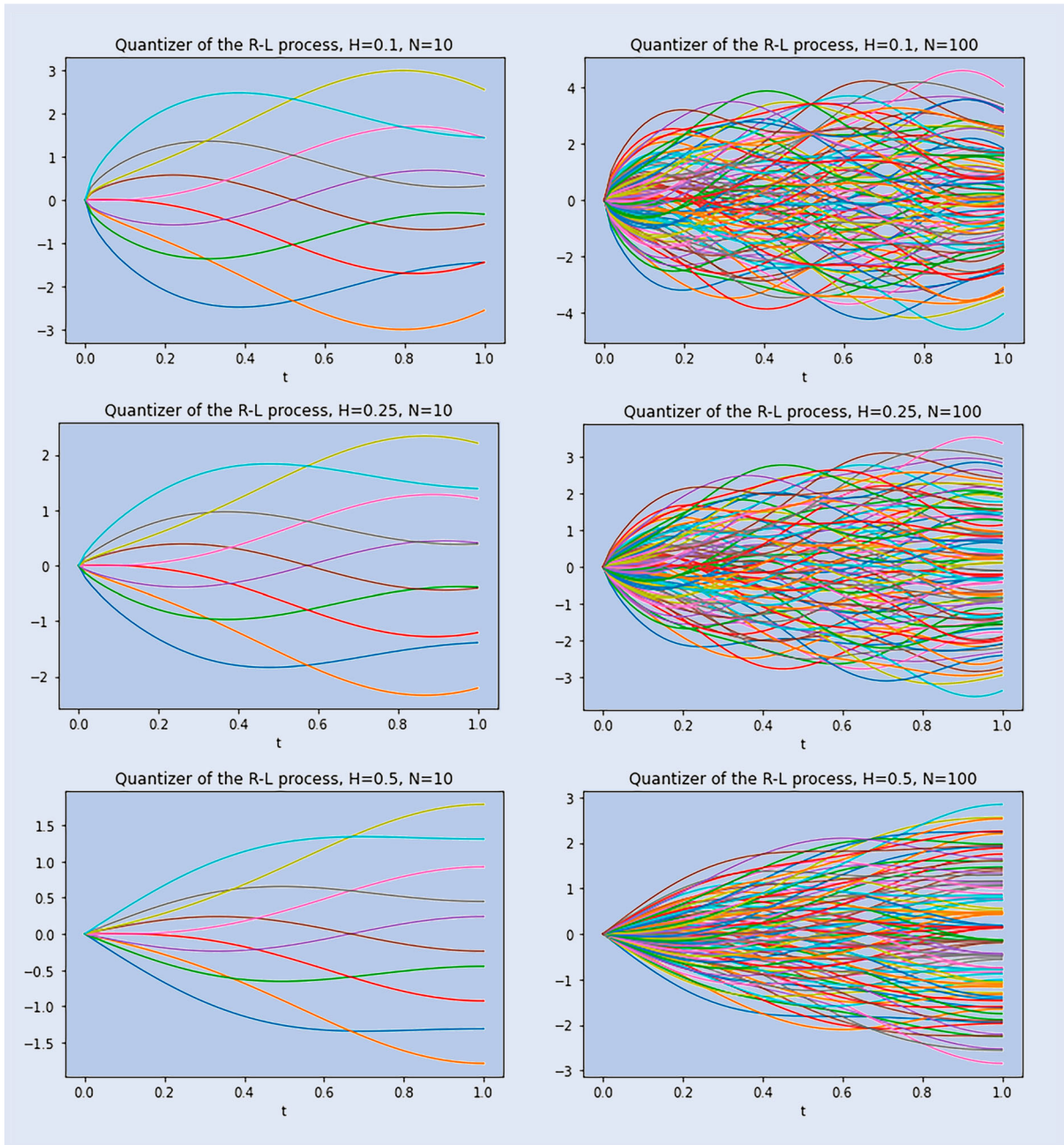
Figure 1. Product functional quantizations of the RL process with N-quantizers, for $H \in \{0.1, 0.25, 0.5\}$, for $N = 10$ and $N = 100$.
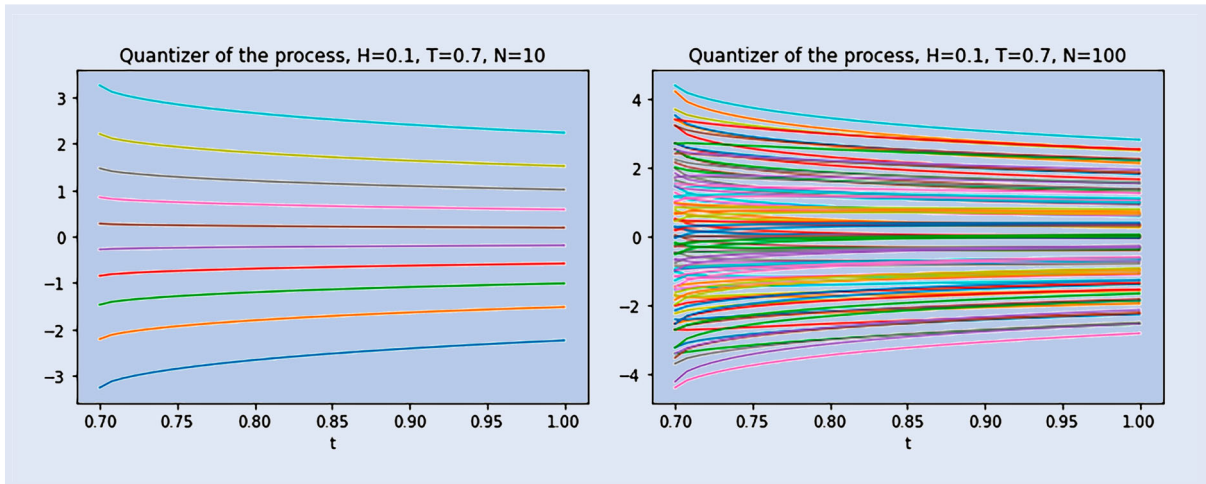

Figure 2. Product functional quantization of $Z^{H,T}$ via N-quantizers, with $H = 0.1$, $T = 0.7$, for $N \in \{10, 100\}$.
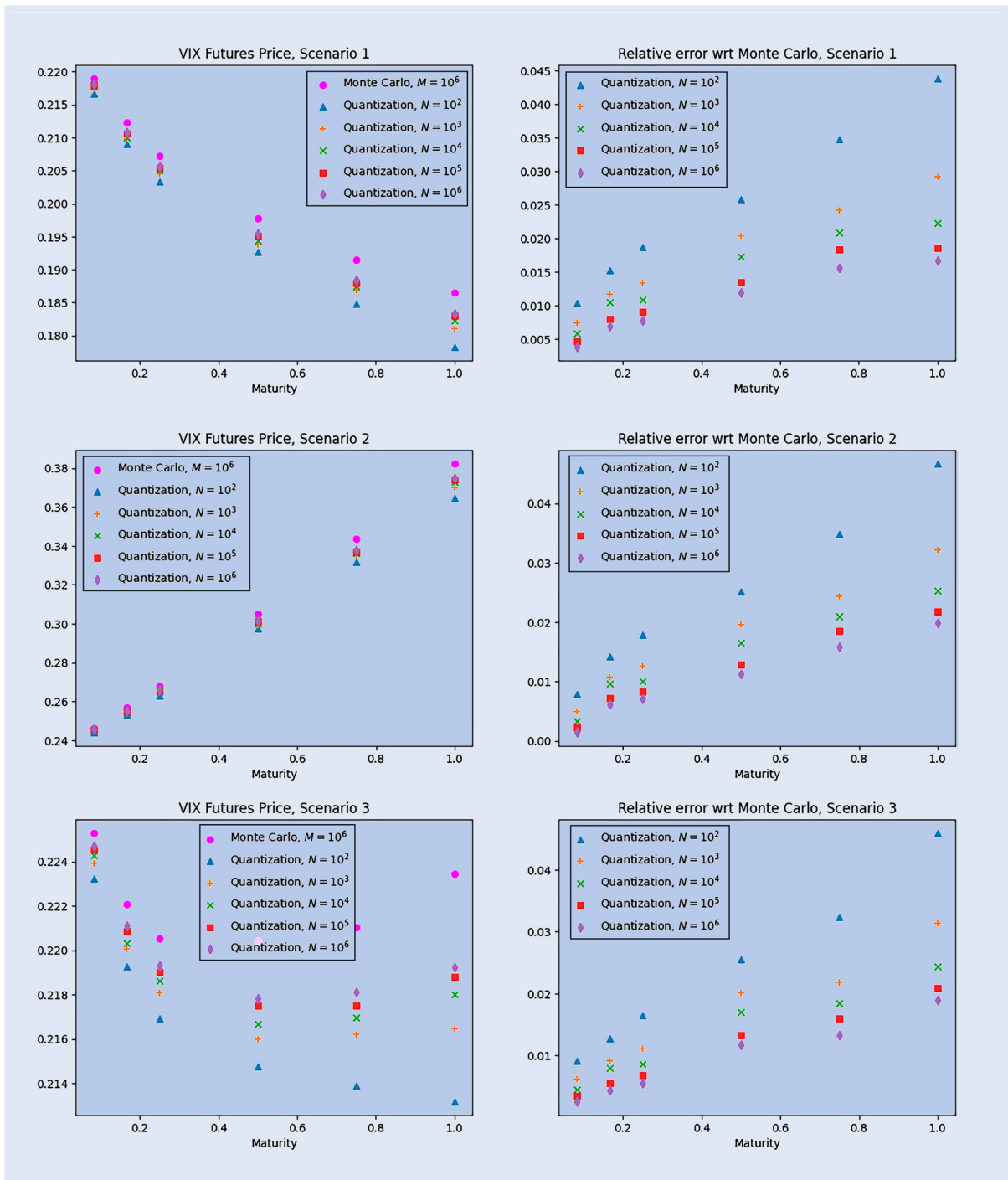
Figure 3. VIX Futures prices (left) and relative error (right) computed with quantization and with Monte-Carlo as a function of the maturity T, for different numbers of trajectories, for each forward variance curve scenario.

Monte Carlo scheme proposed here.† For the sake of completeness, we also recall that combining Monte Carlo pricing of VIX futures/options with an efficient control variate speeds up the computations significantly (Horvath *et al.* 2020).

In figure 4, we show some plots comparing the behavior of the empirical error with the theoretically predicted one.

We have decided to display only a couple of maturities for the first scenario since the other plots are very similar. The figures display in a clear way that the order of convergence of the empirical error should be bigger than the theoretically predicted one: in particular, we expect it to be $\mathcal{O}(\log(N)^{-1})$.

5.3.2. VIX options pricing. To complete the discussion on VIX Options pricing, we present in figure 5 the approximation of the prices of ATM Call Options on the VIX obtained via quantization as a function of the maturity T and for different numbers of trajectories against the same price computed via

---

† The computer used to run the Monte Carlo codes is a virtual machine (OpenStack/Nova/KVM/Qemu, www.openstack.org) with the following technical specifications: RAM: 32.00 GB, CPU: 8 virtual cores, Hypervisor CPU: Intel(R) Xeon(R) CPU E5-2650 v3 @ 2.30GHz, RAM 128GB, Storage: CEPH cluster (www.ceph.com).

Table 3. Grid organization times (in seconds) as a function of the maturity (rows, in months) and of the number of trajectories (columns).

	Grid organization time				
	10^2	10^3	10^4	10^5	10^6
1	0.474	0.491	0.99	4.113	37.183
2	0.476	0.487	0.752	4.294	39.134
3	0.617	0.536	0.826	4.197	37.744
6	0.474	0.475	0.787	4.432	37.847
9	0.459	0.6	0.858	3.73	41.988
12	0.498	0.647	1.016	3.995	38.045
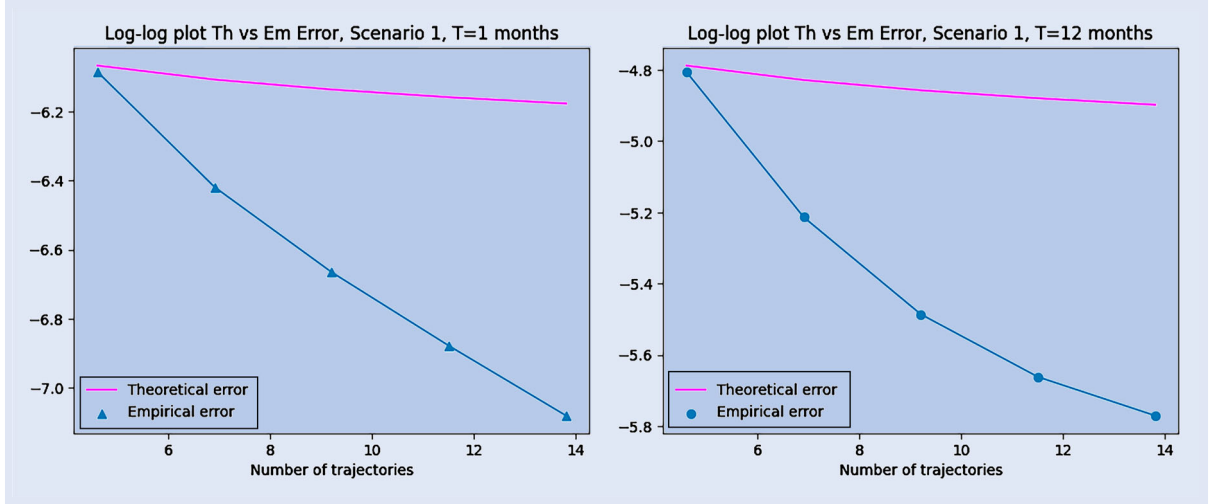
Figure 4. Log–log (natural logarithm) plot of the empirical absolute error with the theoretically predicted one for scenario 1, with $T \in \{1, 12\}$ months.

Monte Carlo simulations with $M = 10^6$ trajectories and 300 equidistant point for the time grid, as a benchmark. Each plot represents a different scenario for the initial forward variance curve. For all scenarios, as the number N of trajectories goes to infinity, the prices in figure 5 are clearly converging, and the limiting curve is increasing in the maturity, as it should be.

5.3.3. Pricing of continuously monitored options on realized variance.
Product functional quantization of the process $(Z_t^H)_{t \in [0,T]}$ can be exploited for (meaningful) pricing purposes, too. We first price variance swaps, whose price is given by the following expression:

$$\mathfrak{S}_T := \mathbb{E}\left[\frac{1}{T}\int_0^T \mathcal{V}_t dt \,\middle|\, \mathcal{F}_0\right].$$

Let us recall that, in the rough Bergomi model,

$$\mathcal{V}_t = v_0(t) \exp\left(2\nu C_H Z_t^H - \frac{\nu^2 C_H^2}{H} t^{2H}\right),$$

where $C_H = \sqrt{\frac{2H\Gamma(3/2-H)}{\Gamma(H+1/2)\Gamma(2-2H)}}$, $\nu > 0$ is an endogenous constant and $v_0(t)$ being the initial forward variance curve. Thus, exploiting the fact that, for any fixed $t \in [0, T]$, Z_t^H is distributed according to a centered Gaussian random variable with variance $\int_0^t (t-s)^{2H-1} ds = \frac{t^{2H}}{2H}$, the quantity $\mathfrak{S}_T$ can be explicitly computed:

$$\mathfrak{S}_T = \frac{1}{T}\int_0^T v_0(t) dt.$$

This is particularly handy and provides us a simple benchmark. The price $\mathfrak{S}_T$ is, then, approximated via quantization through

$$\widehat{\mathfrak{S}}_T^{\mathbf{d}} = \sum_{i \in I^d} \left(\frac{1}{T}\int_0^T v_0(t) \exp\left(2\nu C_H \sum_{n=1}^m \mathcal{K}_H[\psi_n](t) x_{i_n}^{d(n)}\right.\right.$$
$$\left.\left. - \frac{\nu^2 C_H^2}{H} t^{2H}\right) dt\right) \prod_{n=1}^m \mathbb{P}(\xi_n \in C_{i_n}(\Gamma^{d(n)})).$$

Numerical results are presented in figure 6. On the left-hand side, we display a table with the approximations (depending on N, the number of trajectories) of the price of a swap on the realized variance in Scenario 1, for $T = 1$, and the true value $v_0 = 0.234^2$. On the right-hand side a log–log (natural logarithm) plot of the error against the function $c \log(N)^{-H}$, with c being a suitable positive constant. For variance swaps the error is not performing very well. It is indeed very close to the upper bound $c \log(N)^{-H}$ that we have computed theoretically. One possible theoretical motivation for this behavior lies in the difference between *strong* and *weak* error rates. Weak error and strong error do not necessarily share the same order of convergence, being the weak error faster in general. See Bayer *et al.* (2021, 2022) and Gassiat (2022) for recent
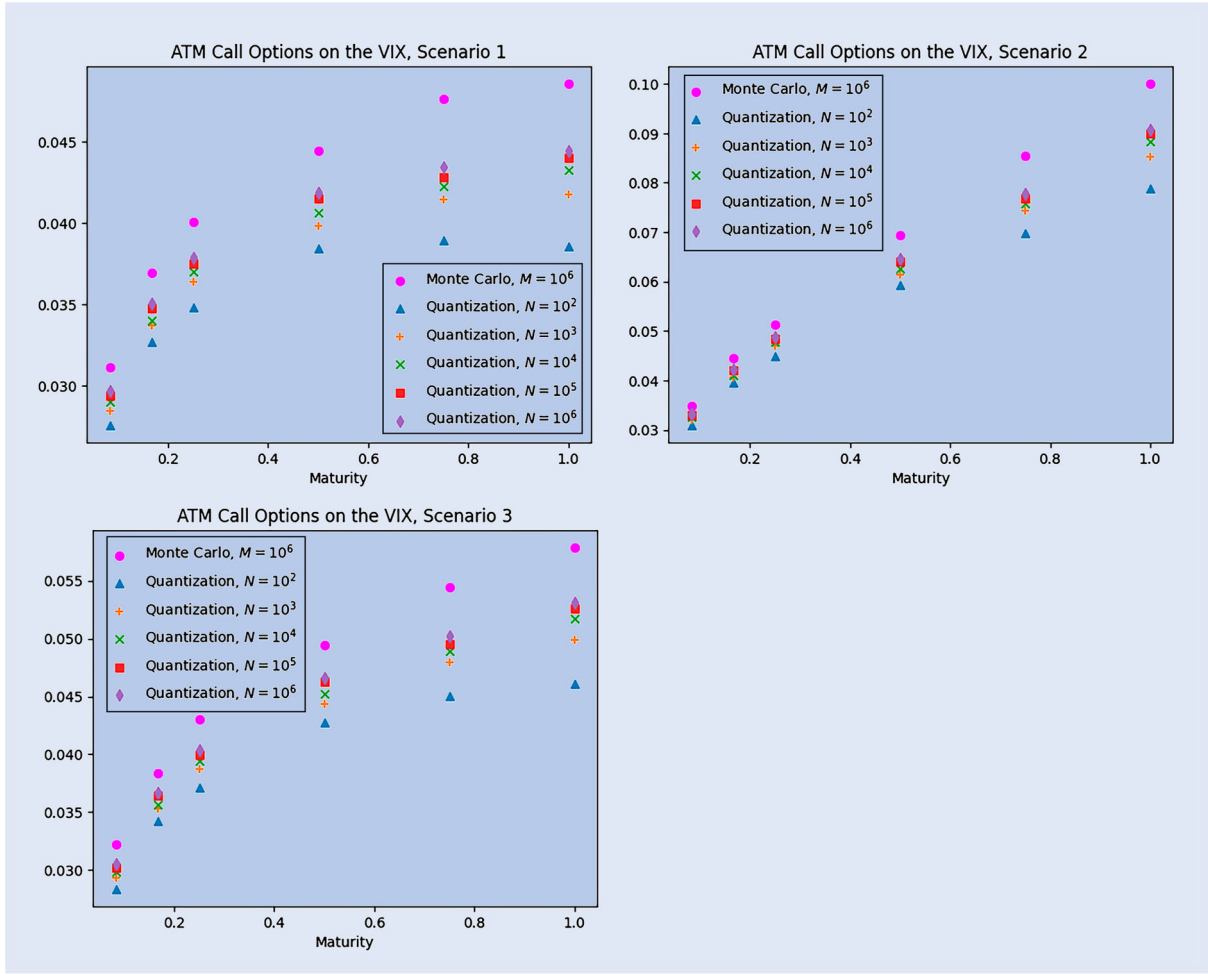
Figure 5. Prices of ATM Call Options on the VIX via quantization.

developments on the topic in the rough volatility framework. For pricing purposes, we are interested in weak error rates. Indeed, the pricing error should in principle have the following form $\mathbb{E}[f(Z^H)] - \mathbb{E}[f(\widehat{Z}^H)]$, where $\widehat{Z}^H$ is the process that we are using to approximate the original Z^H and f is a functional that comes from the payoff function and that we can interpret as a test function. Thus the functional f has a smoothing effect. On the other hand, the upper bound for the quantization error we have computed is a strong error rate. This theoretical discrepancy motivates the findings in figure 4 when pricing VIX Futures and other options on the VIX: the empirical error seems to converge with order $\mathcal{O}(\log(N)^{-1})$, while the predicted order is $\mathcal{O}(\log(N)^{-H})$. The different empirical rates that are seen in figure 4 for VIX futures (roughly $\mathcal{O}(\log(N)^{-1})$)) and in figure 6 for variance swaps (much closer to $\mathcal{O}(\log(N)^{-H})$) could be also related to the different degree of pathwise regularity of the processes Z and Z^T. While $t \to Z_t = \int_0^t K(t-s)\, dWs$ is a.s. $(H-\epsilon)$-Hölder, for fixed T, the trajectories $t \to Z_t^T = \int_0^T K(t-s)\, dWs$ of Z^T are much smoother when $t \in (T, T + \Delta)$ and t is bounded away from T. When pricing VIX derivatives, we are quantizing almost everywhere a smooth Gaussian process (hence error rate of order $\log(N)^{-1}$), while when pricing derivatives on realized variance, we are applying quantization to a rough Gaussian process (hence error rate of order $\mathcal{O}(\log(N)^{-H})$), resulting in a deteriorated accuracy for the prices of

realized volatility derivatives such as the variance swaps in figure 6.

Furthermore, it can be easily shown that, for any $\mathbf{d} \in \mathcal{D}_m^N$ and for any $m, N \in \mathbb{N}$, with $m < N$, $\widehat{\mathfrak{S}}_T^{\mathbf{d}}$ always provides a lower bound for the true price $\mathfrak{S}_T$. Indeed, since the quantizers $\widehat{Z}^{H,\mathbf{d}}$ of the process Z^H are stationary (cfr. proposition 3.12), an application of remark 3.9 to the convex function $f(x) = \exp(2\nu C_H x)$ together with the positivity of $v_0(t) \exp(-\frac{\nu^2 C_H^2 t^{2H}}{H})$, for any $t \in [0, T]$, yields

$$
\begin{aligned}
\widehat{\mathfrak{S}}_T^{\mathbf{d}} &= \mathbb{E}\left[\frac{1}{T} \int_0^T v_0(t) \exp\left(-\frac{\nu^2 C_H^2 t^{2H}}{H} \right) \right. \\
&\quad \left. \times \exp\left(2\nu C_H \widehat{Z}_T^{H,\mathbf{d}} \right) dt \,\middle|\, \mathcal{F}_0 \right] \\
&= \frac{1}{T} \int_0^T v_0(t) \exp\left(-\frac{\nu^2 C_H^2 t^{2H}}{H} \right) \\
&\quad \times \mathbb{E}_0\left[\exp\left(2\nu C_H \widehat{Z}_T^{H,\mathbf{d}} \right) \right] dt \\
&\le \frac{1}{T} \int_0^T v_0(t) \exp\left(-\frac{\nu^2 C_H^2 t^{2H}}{H} \right) \\
&\quad \times \mathbb{E}_0\left[\exp\left(2\nu C_H Z_T^H \right) \right] dt = \mathfrak{S}_T.
\end{aligned}
$$

To complete this section, we plot in figure 7 approximated prices of European Call Options on the realized variance

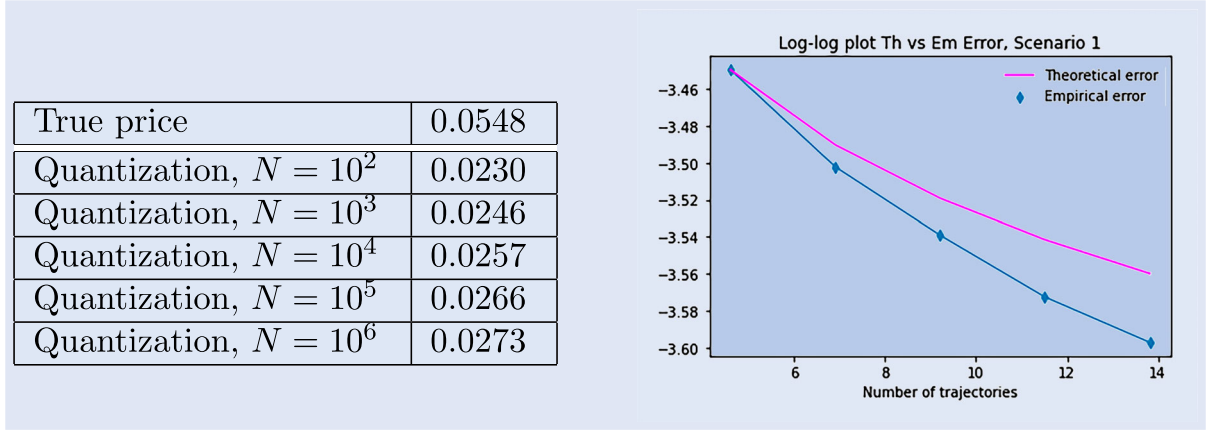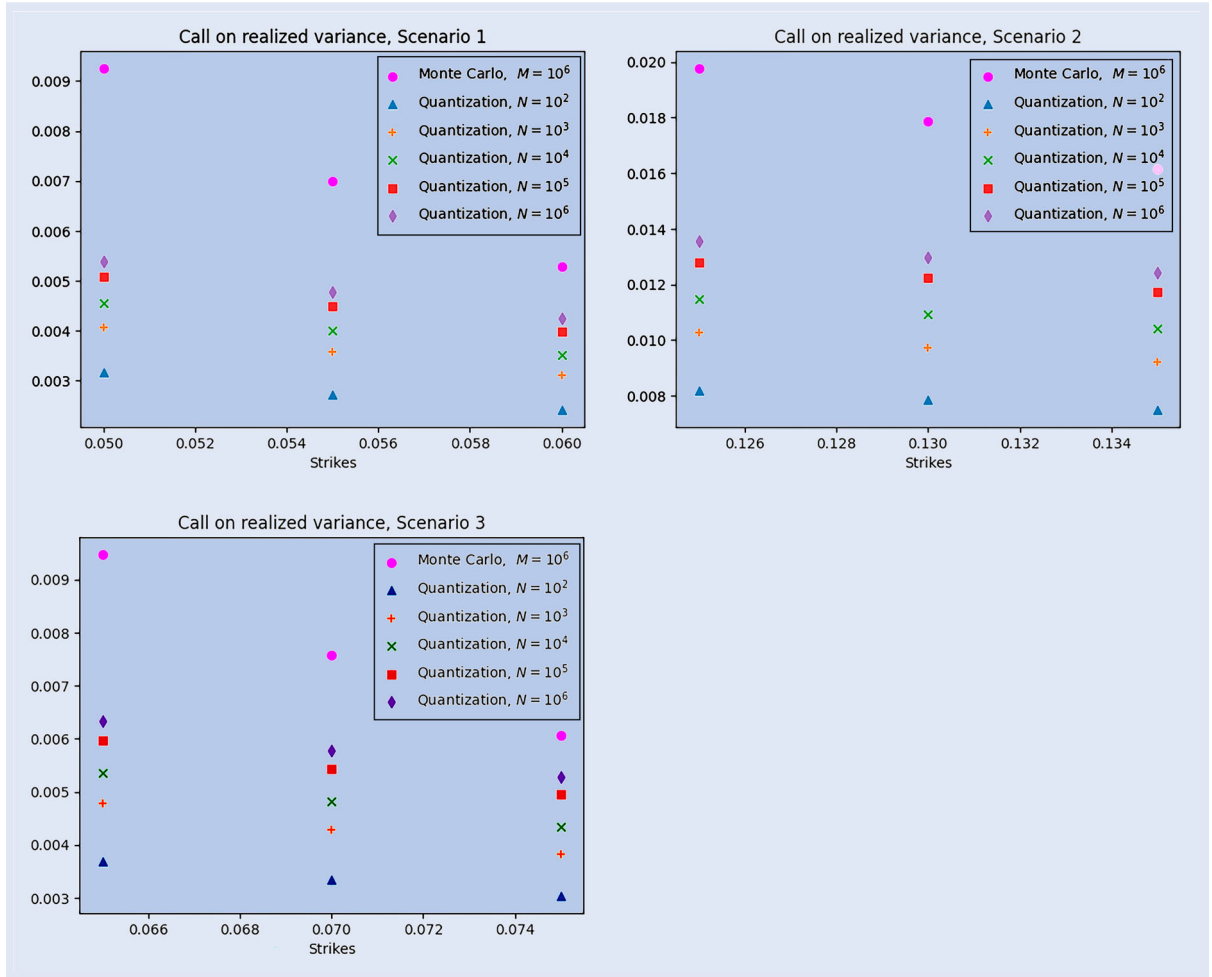| True price	0.0548
Quantization, $N = 10^2$	0.0230
Quantization, $N = 10^3$	0.0246
Quantization, $N = 10^4$	0.0257
Quantization, $N = 10^5$	0.0266
Quantization, $N = 10^6$	0.0273

Figure 6. Prices and errors for variance swaps.

Figure 7. Prices of European Call Option on realized variance computed via Monte Carlo with $M = 10^6$ trajectories and via quantization with $N \in \{10^2, 10^3, 10^4, 10^5, 10^6\}$ trajectories, as a function of K.

via quantization with $N \in \{10^2, 10^3, 10^4, 10^5, 10^6\}$ trajectories and via Monte Carlo with $M = 10^6$ trajectories, as a benchmark. In order to take advantage of the trajectories obtained, we compute the price of a realized variance Call option with strike K and maturity $T = 1$ as

$$\mathcal{C}(K, T) = \mathbb{E}\left[\left(\frac{1}{T} \int_0^T \mathcal{V}_t \mathrm{d}t - K \right)_+ \Bigg| \mathcal{F}_0 \right],$$

and we approximate it via quantization through

$$\widehat{\mathcal{C}^{\mathbf{d}}}(K, T) = \sum_{\underline{i} \in I^d} \left(\frac{1}{T} \int_0^T v_0(t) \exp\left(2\nu C_H \sum_{n=1}^m \mathcal{K}_H[\psi_n](t) x_{i_n}^{d(n)} \right. \right.$$

$$\left. \left. - \frac{\nu^2 C_H^2}{H} t^{2H} \right) \mathrm{d}t - K \right)_+ \prod_{n=1}^m \mathbb{P}(\xi_n \in C_{i_n}(\Gamma^{d(n)})).$$
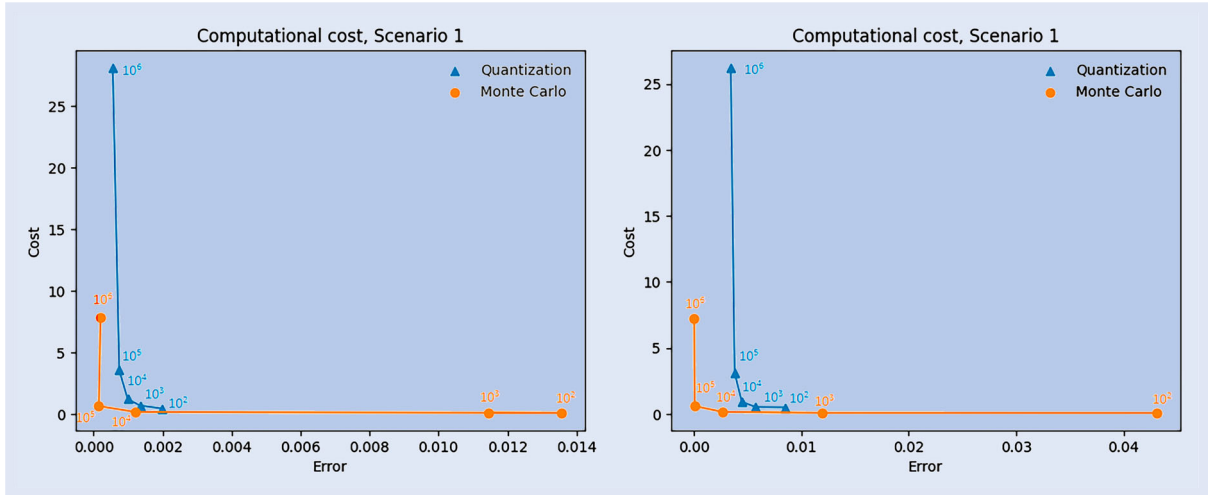
Figure 8. Computational costs for quantization versus Monte Carlo for Scenario 1, with $T = 1$ month (left-hand side) and $T = 12$ months (right-hand side). The number of trajectories, M for Monte Carlo and N for quantization, corresponding to a specific dot is displayed above it.

The three plots in figure 7 display the behavior of the price of a European Call on the realized variance as a function of the strike price K (close to the ATM value) for the three scenarios considered before.

5.3.4. Quantization and MC comparison.
To make a fair comparison between quantization and Monte Carlo simulations, we present a figure to display, for each methodology, the computational work needed for a given error tolerance for the pricing of VIX Futures. The plots in figure 8 should be read as follows. First, for any $M, N \in \{10^2, 10^3, 10^4, 10^5, 10^6\}$, we have computed the corresponding pricing errors: $\varepsilon^{MC}(M) := |\text{Price}^{MC}(M) - \text{RefPrice}|$ and $\varepsilon^{Q}(N) := |\text{Price}^{Q}(N) - \text{RefPrice}|$ where $\text{Price}^{MC}(M)$ is the Monte Carlo price obtained via truncated Cholesky with M trajectories, $\text{Price}^{Q}(N)$ is the price computed via quantization with N trajectories and RefPrice comes from the lowerbound in equation (3.4) in Jacquier *et al.* (2018a) and the associated computational time in seconds $t^{MC}(M)$ and $t^{Q}(N)$, respectively for Monte Carlo simulation and quantization. Then, each point in the plot is associated either to a value of M in case of Monte Carlo (the circles in figure 8), or N in case of quantization (the triangles in figure 8), and its x-coordinate provides the absolute value of the associated pricing error, while its y-coordinate represents the associated computational cost in seconds.

These plots lead to the following observations:

- For quantization, which is an exact method, the error is strictly monotone in the number of trajectories.
- When a small number of trajectories is considered, quantization provides a lower error with respect to Monte Carlo, at a comparable cost.
- For large numbers of trajectories Monte Carlo overcomes quantization both in terms of accuracy and of computational time.

To conclude, quantization can always be run with an arbitrary number of trajectories and furthermore for $N \in$ $\{10^2, 10^3, 10^4\}$ it leads to a lower error with respect to Monte Carlo, at a comparable computational cost, as it is visible from figure 8. This makes quantization particularly suitable to be used when dealing with standard machines, i.e. laptops with a RAM memory smaller or equal to 16GB.

6. Conclusion

In this paper we provide, on the theoretical side, a precise and detailed result on the convergence of product functional quantizers of *Gaussian Volterra processes*, showing that the L^2-error is of order $\log(N)^{-H}$, with N the number of trajectories and H the regularity index.

Furthermore, we explicitly characterize the rate optimal parameters, m_N^* and $\mathbf{d}_N^*$, and we compare them with the corresponding optimal parameters, $\overline{m}_N$ and $\overline{\mathbf{d}}_N$, computed numerically.

In the rough Bergomi model, we apply product functional quantization to the pricing of VIX options, with precise rates of convergence, and of options on realized variance, comparing those—whenever possible—to standard Monte Carlo methods.

The thorough numerical analysis carried out in the paper shows that unfortunately, despite the conceptual promise of functional quantization, while the results on the VIX are very promising, other types of path-dependent options seem to require machine resources way beyond the current requirements of standard Monte Carlo schemes, as shown precisely in the case of variance swaps. While product functional quantization is an exact method, the analysis provided here does not however promise a bright future in the context of rough volatility. It may nevertheless be of practical interest when machine resources are limited and indeed the results for VIX Futures pricing are strongly encouraging in this respect. Functional quantization for rough volatility can, however, be salvaged when used as a control variate tool to reduce the variance in classical Monte Carlo simulations.

Acknowledgments

Disclosure statement

No potential conflict of interest was reported by the author(s).

Funding

ORCID

G. Callegaro http://orcid.org/0000-0001-9026-5261

References

Abi Jaber, E. and El Euch, O., Multifactor approximation of rough volatility models. *SIAM J. Financ. Math.*, 2019, **10**(2), 309–349.

Adler, R.J. and Taylor, J.E., *Random Fields and Geometry*. Springer Monographs in Mathematics, 2007 (Springer-Verlag: New York).

Alòs, E., León, J.A. and Vives, J., On the short-time behavior of the implied volatility for jump-diffusion models with stochastic volatility. *Finance Stoch.*, 2007, **11**(4), 571–589.

Bayer, C., Friz, P.K. and Gatheral, J., Pricing under rough volatility. *Quant. Finance*, 2016, **16**(6), 887–904.

Bayer, C., Hammouda, C.B. and Tempone, R., Hierarchical adaptive sparse grids and quasi Monte Carlo for option pricing under the rough Bergomi model. *Quant. Finance*, 2020, **20**(9), 1457–1473.

Bayer, C., Hall, E.J. and Tempone, R., Weak error rates for option pricing under linear rough volatility, arXiv preprint, 2021. https://arxiv.org/abs/2009.01219.

Bayer, C., Fukasawa, M. and Nakahara, S., On the weak convergence rate in the discretization of rough volatility models, ArXiV preprint, 2022. https://arxiv.org/abs/2203.02943.

Bennedsen, M., Lunde, A. and Pakkanen, M.S., Hybrid scheme for Brownian semistationary processes. *Finance Stoch.*, 2017, **21**, 931–965.

Bergomi, L., Smile dynamics II, Risk, 2005, pp. 67–73.

Carr, P.P. and Madan, D.B., Joint modeling of VIX and SPX options at a single and common maturity with risk management applications. *IIE Trans.*, 2014, **46**(11), 1125–1131.

Chen, W., Langrené, N., Loeper, G. and Zhu, Q., Markovian approximation of the rough Bergomi model for Monte Carlo option pricing. *Mathematics*, 2021, **9**(5), 528.

Chow, Y.S. and Teichner, E., *Probability Theory*. Springer Texts in Statistics, 1997 (Springer-Verlag: New York).

Corlay, S., Quelques aspects de la quantification optimale, et applications en finance (in English, with French summary). PhD Thesis, Université Pierre et Marie Curie, 2011.

Fukasawa, M., Asymptotic analysis for stochastic volatility: Martingale expansion. *Finance Stoch.*, 2011, **15**(4), 635–654.

Fukasawa, M., Volatility has to be rough. *Quant. Finance*, 2021, **21**, 1–8.

Fukasawa, M., Takabatake, T. and Westphal, R., Consistent estimation for fractional stochastic volatility model under high-frequency asymptotics (Is Volatility Rough?). *Math. Finance.*, 2022, **32**, 1086–1132.

Gassiat, P., Weak error rates of numerical schemes for rough volatility, arXiv preprint, 2022. https://arxiv.org/abs/2203.09298.

Gatheral, J., *Consistent Modelling of SPX and VIX Options*. Presentation, 2008 (Bachelier Congress: London).

Gatheral, J., Jaisson, T. and Rosenbaum, M., Volatility is rough. *Quant. Finance*, 2018, **18**(6), 933–949.

Gersho, A. and Gray, R.M., *Vector Quantization and Signal Compression*, 1992 (Kluwer Academic Publishers: New York).

Graf, S. and Luschgy, H., *Foundations of Quantization for Probability Distributions*. Lecture Notes in Mathematics, 1730, 2007 (Springer: Berlin Heidelberg).

Horvath, B., Jacquier, A. and Muguruza, A., Functional central limit theorems for rough volatility, 2019. arxiv.org/abs/1711.03078.

Horvath, B., Jacquier, A. and Tankov, P., Volatility options in rough volatility models. *SIAM J. Financ. Math.*, 2020, **11**(2), 437–469.

Huh, J., Jeon, J. and Kim, J.H., A scaled version of the double-mean-reverting model for VIX derivatives. *Math. Financ. Econom.*, 2018, **12**(4), 495–515.

Jacquier, A., Martini, C. and Muguruza, A., On VIX futures in the rough Bergomi model. *Quant. Finance*, 2018a, **18**(1), 45–61.

Jacquier, A., Pakkanen, M.S. and Stone, H., Pathwise large deviations for the rough Bergomi model. *J. Appl. Probab.*, 2018b, **55**(4), 1078–1092.

Kallenberg, O., *Foundations of Modern Probability*. 2nd edn, Probability and Its Applications, 2002 (Springer-Verlag: New York).

Karp, D.B., Representations and inequalities for generalized Hypergeometric functions. *J. Math. Sci. (N.Y.)*, 2015, **207**, 885–897.

Kokholm, T. and Stisen, M., Joint pricing of VIX and SPX options with stochastic volatility and jump models. *J. Risk Finance*, 2015, **16**(1), 27–48.

Luke, Y.L., *The Special Functions and Their Approximations*, Vol. 1, 1969 (Academic Press: New York and London).

Luschgy, H. and Pagès, G., Functional quantization of Gaussian processes. *J. Funct. Anal.*, 2002, **196**(2), 486–531.

Luschgy, H. and Pagès, G., High-resolution product quantization for Gaussian processes under sup-norm distortion. *Bernoulli*, 2007, **13**(3), 653–671.

McCrickerd, R. and Pakkanen, M.S., Turbocharging Monte Carlo pricing for the rough Bergomi model. *Quant. Finance*, 2018, **18**(11), 1877–1886.

Olver, F.W.J., *Asymptotics and Special Functions*, 2nd ed., 1997 (A.K. Peters/CRC Press: New York).

Pagès, G., Quadratic optimal functional quantization of stochastic processes and numerical applications. In *Monte Carlo and Quasi-Monte Carlo Methods 2006*, pp. 101–142, 2007 (Springer: Berlin Heidelberg).

Pagès, G. and Printems, J., Functional quantization for numerics with an application to option pricing. *Monte Carlo Methods Appl.*, 2005, **11**(4), 407–446.

Picard, J., Representation formulae for the fractional Brownian motion. In *Séminaire de Probabilités XLIII*, Lecture Notes in Mathematics, 2006, pp. 3–70, 2011 (Springer-Verlag: Berlin Heidelberg).

Sheppard, W.F., On the calculation of the most probable values of frequency-constants, for data arranged according to equidistant division of a scale. *Proc. Lond. Math. Soc. (3)*, 1897, **1**(1), 353–380.

Steele, J.M., *The Cauchy-Schwarz Master-Class*, 2004 (Cambridge University Press: New York).

Appendices

Appendix 1. Proofs

A.1. *Proof of proposition 3.6*

Consider a fixed $N \geq 1$ and $(m, \mathbf{d})$ for $\mathbf{d} \in \mathcal{D}_m^N$. We have

$$
\mathbb{E}\left[\left\|Z - \widehat{Z}^{\mathbf{d}}\right\|_{L^2[0,1]}^2\right]
$$

$$
= \mathbb{E}\left[\left\|\sum_{n\geq 1}\mathcal{K}[\psi_n](\cdot)\xi_n - \sum_{n=1}^m \mathcal{K}[\psi_n](\cdot)\widehat{\xi}_n^{d(n)}\right\|_{L^2[0,1]}^2\right]
$$

$$
= \mathbb{E}\left[\left\|\sum_{n=1}^m \mathcal{K}[\psi_n](\cdot)(\xi_n - \widehat{\xi}_n^{d(n)}) + \sum_{k\geq m+1}\mathcal{K}[\psi_k](\cdot)\xi_k\right\|_{L^2[0,1]}^2\right]
$$

$$
= \mathbb{E}\left[\int_0^1 \left|\sum_{n=1}^m \mathcal{K}[\psi_n](t)(\xi_n - \widehat{\xi}_n^{d(n)}) + \sum_{k\geq m+1}\mathcal{K}[\psi_k](t)\xi_k\right|^2 dt\right]
$$

$$
= \int_0^1 \left(\sum_{n=1}^m \mathcal{K}[\psi_n]^2(t)\mathbb{E}\left[|\xi_n - \widehat{\xi}_n^{d(n)}|^2\right] + \sum_{k\geq m+1}\mathcal{K}[\psi_k]^2(t)\right) dt
$$

$$
= \int_0^1 \left(\sum_{n=1}^m \mathcal{K}[\psi_n]^2(t)\boldsymbol{\varepsilon}^{d(n)}(\xi_n)^2 + \sum_{k\geq m+1}\mathcal{K}[\psi_k]^2(t)\right) dt,
$$
(A1)

using Fubini's Theorem and the fact that $\{\xi_n\}_{n\geq 1}$ is a sequence of i.i.d. Gaussian and where $\boldsymbol{\varepsilon}^{d(n)}(\xi_n) := \inf_{(\alpha_1,\ldots,\alpha_{d(n)})\in\mathbb{R}^{d(n)}}$ $\sqrt{\mathbb{E}[\min_{1\leq i\leq d(n)}|\xi_n - \alpha_i|^2]}$. The Extended Pierce Lemma (Pagès 2007, theorem 1(b)) ensures that $\boldsymbol{\varepsilon}^{d(n)}(\xi_n) \leq \frac{L}{d(n)}$ for a suitable positive constant L. Exploiting this error bound and the property (B) for $\mathcal{K}[\psi_n]$ in assumption 2.3, we obtain

$$
\mathbb{E}\left[\|Z - \widehat{Z}^{\mathbf{d}}\|_{L^2[0,1]}^2\right]
$$

$$
= \sum_{n=1}^m \left(\int_0^1 \mathcal{K}[\psi_n]^2(t)\,dt\right)\boldsymbol{\varepsilon}^{d(n)}(\xi_n)^2 + \sum_{k\geq m+1}\int_0^1 \mathcal{K}[\psi_k]^2(t)\,dt
$$

$$
\leq C_2^2 \left\{\sum_{n=1}^m n^{-(2H+1)}\boldsymbol{\varepsilon}^{d(n)}(\xi_n)^2 + \sum_{k\geq m+1}k^{-(2H+1)}\right\}
$$

$$
\leq C_2^2 \left\{\sum_{n=1}^m n^{-(2H+1)}\frac{L^2}{d(n)^2} + \sum_{k\geq m+1}k^{-(2H+1)}\right\}
$$

$$
\leq \widetilde{C}\left(\sum_{n=1}^m \frac{1}{n^{2H+1}d(n)^2} + \sum_{k\geq m+1}k^{-(2H+1)}\right),
$$
(A2)

with $\widetilde{C} = \max\{L^2 C_2^2, C_2^2\}$. Inspired by Luschgy and Pagès (2002, section 4.1), we now look for an 'optimal' choice of $m \in \mathbb{N}$ and $\mathbf{d} \in \mathcal{D}_m^N$. This reduces the error in approximating Z with a product quantization of the form in (9). Define the optimal product functional quantization $\widehat{Z}^{N,\star}$ of order N as the $\widehat{Z}^{\mathbf{d}}$ which realizes the minimal error:

$$
\mathbb{E}\left[\left\|Z - \widehat{Z}^{N,\star}\right\|_{L^2[0,1]}^2\right]
$$

$$
= \min\left\{\mathbb{E}\left[\left\|Z - \widehat{Z}^{\mathbf{d}}\right\|_{L^2[0,1]}^2\right], m \in \mathbb{N}, \mathbf{d} \in \mathcal{D}_m^N\right\}.
$$

From (A2), we deduce

$$
\mathbb{E}\left[\left\|Z - \widehat{Z}^{N,\star}\right\|_{L^2[0,1]}^2\right]
$$

$$
\leq \widetilde{C}\inf_{m\in\mathbb{N}}\left\{\sum_{k\geq m+1}\frac{1}{k^{2H+1}} + \inf\left\{\sum_{n=1}^m \frac{1}{n^{2H+1}d(n)^2}, \mathbf{d}\in\mathcal{D}_m^N\right\}\right\}.
$$
(A3)

For any fixed $m \in \mathbb{N}$, we associate to the internal minimization problem the one we get by relaxing the hypothesis that $d(n) \in \mathbb{N}$:

$$
\mathfrak{I} := \inf\left\{\sum_{n=1}^m \frac{1}{n^{2H+1}z(n)^2}, \{z(n)\}_{n=1,\ldots,m} \in (0,\infty) : \prod_{n=1}^m z(n) \leq N\right\}.
$$

For this infimum, we derive a simple solution exploiting the arithmetic-geometric inequality using lemma A.3. Setting $\widetilde{z}(n) := \gamma_{N,m}n^{-(H+\frac{1}{2})}$, with $\gamma_{N,m} := N^{\frac{1}{m}}(\prod_{j=1}^m j^{-(2H+1)})^{-\frac{1}{2m}}$, $n = 1,\ldots,m$, we get

$$
\mathfrak{I} = \sum_{n=1}^m \frac{1}{n^{2H+1}\widetilde{z}(n)^2} = N^{-\frac{2}{m}}m\left(\prod_{n=1}^m n^{-(2H+1)}\right)^{\frac{1}{m}},
$$

and note that the sequence $\{\widetilde{z}(n)\}$ is decreasing. Since ultimately the vector $\mathbf{d}$ consists of integers, we use $\widetilde{d}(n) = \lfloor\widetilde{z}(n)\rfloor$, $n = 1,\ldots,m$. In fact, this choice guarantees that

$$
\prod_{n=1}^m \widetilde{d}(n) = \prod_{n=1}^m \lfloor\widetilde{z}(n)\rfloor \leq \prod_{n=1}^m \widetilde{z}(n) = N.
$$

Furthermore, setting $\widetilde{d}(j) = \lfloor\widetilde{z}(j)\rfloor$ for each $j \in \{1,\ldots,m\}$, we obtain

$$
\frac{\widetilde{d}(j)+1}{(j^{-(2H+1)})^{\frac{1}{2}}} = j^{H+\frac{1}{2}}(\lfloor\widetilde{z}(j)\rfloor + 1)
$$

$$
\geq j^{H+\frac{1}{2}}\widetilde{z}(j) = \frac{j^{H+\frac{1}{2}}N^{\frac{1}{m}}}{j^{H+\frac{1}{2}}}\left\{\prod_{n=1}^m \frac{1}{n^{2H+1}}\right\}^{-\frac{1}{2m}}
$$

$$
= N^{\frac{1}{m}}\left\{\prod_{n=1}^m \frac{1}{n^{2H+1}}\right\}^{-\frac{1}{2m}}.
$$

Ordering the terms, we have $(\widetilde{d}(j)+1)^2 N^{-\frac{2}{m}}(\prod_{n=1}^m n^{-(2H+1)})^{\frac{1}{m}} \geq j^{-(2H+1)}$, for each $j \in \{1,\ldots,m\}$. From this we deduce the following inequality (notice that the left-hand side term is defined only if $\widetilde{d}(1),\ldots,\widetilde{d}(m) > 0$):

$$
\sum_{j=1}^m j^{-(2H+1)}\widetilde{d}(j)^{-2} \leq \sum_{j=1}^m \left(\frac{\widetilde{d}(j)+1}{\widetilde{d}(j)}\right)^2 N^{-\frac{2}{m}}\left(\prod_{n=1}^m n^{-(2H+1)}\right)^{\frac{1}{m}}
$$

$$
= N^{-\frac{2}{m}}\left(\prod_{n=1}^m n^{-(2H+1)}\right)^{\frac{1}{m}}\sum_{j=1}^m \left(\frac{\widetilde{d}(j)+1}{\widetilde{d}(j)}\right)^2
$$

$$
\leq 4mN^{-\frac{2}{m}}\left(\prod_{n=1}^m n^{-(2H+1)}\right)^{\frac{1}{m}}.
$$
(A4)

Hence, we are able to make a first error estimation, placing in the internal minimization of the right-hand side of (A3) the result of inequality in (A4).

$$
\mathbb{E}\left[\left\|Z - \widehat{Z}^{N,\star}\right\|_{L^2[0,1]}^2\right]
$$

$$
\leq \widetilde{C}\inf\left\{\sum_{k\geq m+1}\frac{1}{k^{2H+1}} + 4mN^{-\frac{2}{m}}\left(\prod_{n=1}^m n^{-(2H+1)}\right)^{\frac{1}{m}}, m \in I(N)\right\}
$$

$$\leq C' \inf \left\{ \sum_{k \geq m+1} \frac{1}{k^{2H+1}} + mN^{-\frac{2}{m}} \left(\prod_{n=1}^{m} n^{-(2H+1)} \right)^{\frac{1}{m}}, m \in I(N) \right\}, \quad \text{(A5)}$$

where $C' = 4\widetilde{C}$ and the set

$$I(N) := \{ m \in \mathbb{N} : N^{\frac{2}{m}} m^{-(2H+1)} \left(\prod_{n=1}^{m} n^{-(2H+1)} \right)^{-\frac{1}{m}} \geq 1 \}, \quad \text{(A6)}$$

which represents all m's such that all $\widetilde{d}(1), \ldots, \widetilde{d}(m)$ are positive integers. This is to avoid the case where $\prod_{i=1}^{m} \widetilde{d}(i) \leq N$ holds only because one of the factors is zero. In fact, for all $n \in \{1, \ldots, m\}$, $\widetilde{d}(n) = \lfloor \widetilde{z}(n) \rfloor$ is a positive integer if and only if $\widetilde{z}(n) \geq 1$. Thanks to the monotonicity of $\{z(n)\}_{n=1,\ldots,m}$, we only need to check that

$$\widetilde{z}(m) = N^{\frac{1}{m}} m^{-(H+\frac{1}{2})} \left(\prod_{n=1}^{m} n^{-(2H+1)} \right)^{-\frac{1}{2m}} \geq 1.$$

First, let us show that $I(N)$, defined in (A6) for each $N \geq 1$, is a non-empty finite set with maximum given by $m^*(N)$ of order $\log(N)$. We can rewrite it as $I(N) = \{m \geq 1 : a_m \leq \log(N)\}$, where

$$a_n = \frac{1}{2} \log \left(\prod_{j=1}^{n} \frac{n^{2H+1}}{j^{2H+1}} \right).$$

We can now verify that the sequence a_n is increasing in $n \in \mathbb{N}$:

$$a_n \leq a_{n+1}$$

$$\iff \sum_{j=1}^{n} \log \left(j^{-(2H+1)} \right) - n \log \left(n^{-(2H+1)} \right)$$

$$\leq \sum_{j=1}^{n+1} \log \left(j^{-(2H+1)} \right) - (n+1) \log \left((n+1)^{-(2H+1)} \right)$$

$$\iff -n \log \left(n^{-(2H+1)} \right)$$

$$\leq \log \left((n+1)^{-(2H+1)} \right) - (n+1) \log \left((n+1)^{-(2H+1)} \right)$$

$$\iff \log \left(n^{-(2H+1)} \right) \geq \log \left((n+1)^{-(2H+1)} \right),$$

which is obviously true. Furthermore the sequence $(a_n)_n$ diverges to infinity since

$$\prod_{j=1}^{n} \frac{n^{(2H+1)}}{j^{(2H+1)}} = n^{(2H+1)n} \prod_{j=1}^{n} \frac{1}{j^{(2H+1)}} \geq n^{(2H+1)n} \prod_{j=2}^{n} \frac{1}{j^{(2H+1)}}$$

$$\geq n^{(2H+1)n} \frac{1}{n^{(2H+1)(n-1)}} \geq n^{(2H+1)}.$$

and $H \in (0, \frac{1}{2})$. We immediately deduce that $I(N)$ is finite and, since $\{1\} \subset I(N)$, it is also non-empty. Hence $I(N) = \{1, \ldots, m^*(N)\}$. Moreover, for all $N \geq 1$, $a_{m^*(N)} \leq \log(N) < a_{m^*(N)+1}$, which implies that $m^*(N) = \mathcal{O}(\log(N))$.

Now, the error estimation in (A5) can be further simplified exploiting the fact that, for each $m \in I(N)$,

$$mN^{-\frac{2}{m}} \left(\prod_{n=1}^{m} n^{-(2H+1)} \right)^{\frac{1}{m}}$$

$$= mm^{-(2H+1)} \left(m^{-(2H+1)} N^{\frac{2}{m}} \left(\prod_{n=1}^{m} n^{-(2H+1)} \right)^{-\frac{1}{m}} \right)^{-1}$$

$$\leq m^{-2H}.$$

The last inequality is a consequence of the fact that $(\prod_{n=1}^{m} n^{-(2H+1)})^{-\frac{1}{m}} \geq 1$ by definition. Hence,

$$\mathbb{E} \left[\|Z - \widehat{Z}^{N,\star}\|_{L^2[0,1]}^2 \right]$$

$$\leq C' \inf \left\{ \sum_{k \geq m+1} \frac{1}{k^{2H+1}} + m^{-2H}, m \in I(N) \right\}, \quad \text{(A7)}$$

for some suitable constant $C' > 0$.

Consider now the sequence $\{b_n\}_{n \in \mathbb{N}}$, given by $b_n = \sum_{k \geq n+1} \frac{1}{k^{2H+1}} + n^{-2H}$. For $n \geq 1$,

$$b_{n+1} - b_n = \sum_{k \geq n+2} \frac{1}{k^{2H+1}} + \frac{1}{(n+1)^{2H}} - \left[\sum_{k \geq n+1} \frac{1}{k^{2H+1}} + \frac{1}{n^{2H}} \right]$$

$$= -\frac{1}{(n+1)^{2H}} + \frac{1}{(n+1)^{2H+1}} - \frac{1}{n^{2H}} \leq 0,$$

so that the sequence is decreasing and the infimum in (A7) is attained at $m = m^*(N)$. Therefore,

$$\mathbb{E} \left[\|Z - \widehat{Z}^{N,\star}\|_{L^2[0,1]}^2 \right] \leq C' \inf \left\{ \sum_{k \geq m+1} \frac{1}{k^{2H+1}} + m^{-2H}, m \in I(N) \right\}$$

$$= C' \left(\sum_{k \geq m^*(N)+1} \frac{1}{k^{2H+1}} + m^*(N)^{-2H} \right)$$

$$ss \leq C' \left(m^*(N)^{-2H-1+1} + m^*(N)^{-2H} \right)$$

$$= 2C' m^*(N)^{-2H} \leq C \log(N)^{-2H}.$$

A.2. *Proof of Remark 2.5*

This can be proved specializing the computations done in Luschgy and Pagès ([2007](#), page 656). Consider an arbitrary index $n \geq 1$. For all $t, s \in [0, 1]$, exploiting assumption 2.3, we have that, for any $\rho \in [0, 1]$,

$$|\mathcal{K}[\psi_n](t) - \mathcal{K}[\psi_n](s)|$$

$$= |\mathcal{K}[\psi_n](t) - \mathcal{K}[\psi_n](s)|^{\rho} |\mathcal{K}[\psi_n](t) - \mathcal{K}[\psi_n](s)|^{1-\rho}$$

$$\leq \left(\sup_{u,v \in [0,1], u \neq v} \frac{|\mathcal{K}[\psi_n](u) - \mathcal{K}[\psi_n](v)|}{|u-v|^{H+\frac{1}{2}}} |t-s|^{H+\frac{1}{2}} \right)^{\rho}$$

$$\times \left(2 \sup_{t \in [0,1]} \mathcal{K}[\psi_n](t) \right)^{1-\rho}$$

$$\leq (C_1 n)^{\rho} (2C_2 n^{-(H+\frac{1}{2})})^{1-\rho} |t-s|^{\rho(H+\frac{1}{2})}$$

$$= C_{\rho} n^{\rho(H+\frac{3}{2})-(H+\frac{1}{2})} |t-s|^{\rho(H+\frac{1}{2})},$$

where $C_{\rho} := C_1^{\rho} (2C_2)^{1-\rho} < \infty$. Therefore

$$[\mathcal{K}[\psi_n]]_{\rho(H+\frac{1}{2})} = \sup_{t \neq s \in [0,1]} \frac{|\mathcal{K}[\psi_n](t) - \mathcal{K}[\psi_n](s)|}{|t-s|^{\rho(H+\frac{1}{2})}}$$

$$\leq C_{\rho} n^{\rho(H+\frac{3}{2})-(H+\frac{1}{2})}. \quad \text{(A8)}$$

Notice that $\rho(H + \frac{3}{2}) - (H + \frac{1}{2}) < -\frac{1}{2}$ when $\rho \in [0, \frac{H}{H+3/2}]$ so that (A8) implies

$$\sum_{n=1}^{\infty} [\mathcal{K}[\psi_n]]_{\rho(H+\frac{1}{2})}^2 \leq C_{\rho}^2 \sum_{n=1}^{\infty} n^{2\rho(H+\frac{3}{2})-2(H+\frac{1}{2})}$$

$$\le C_\rho^2 \sum_{n=1}^{\infty} n^{-(1+\varepsilon)} = K < \infty.$$

In particular,

$$\mathbb{E}\left[|Y_t - Y_s|^2\right] = \sum_{n=1}^{\infty} |\mathcal{K}[\psi_n](t) - \mathcal{K}[\psi_n](s)|^2$$

$$\le \sum_{n=1}^{\infty} [\mathcal{K}[\psi_n]]_{\rho(H+\frac{1}{2})}^2 |t-s|^{2\rho(H+\frac{1}{2})}$$

$$\le K|t-s|^{2\rho(H+\frac{1}{2})}.$$

As noticed in Remark 2.2 the process Y is centered Gaussian. Hence, for each $t, s \in [0, 1]$ so is $Y_t - Y_s$. Proposition A.2 therefore implies that, for any $r \in \mathbb{N}$,

$$\mathbb{E}\left[|Y_t - Y_s|^{2r}\right] = \mathbb{E}\left[|Y_t - Y_s|^2\right]^r (2r-1)!! \le K'|t-s|^{2r\rho(H+\frac{1}{2})},$$

where $K' = K^r(2r-1)!!$, yielding existence of a continuous version of Y since choosing $r \in \mathbb{N}$ such that $2r\rho(H+\frac{1}{2}) > 1$, Kolmogorov continuity theorem (Kallenberg 2002, theorem 3.23) applies directly.

A.3. *Proof of Lemma 4.5*

Let $H_+ := H + \frac{1}{2}$. Using Karp (2015, corollary 1, equation (12)) (with $\psi = b_2 + b_1 - a > 1/2$), the identity

$${}_1F_2(a, b_1, b_2, -r) = \frac{\Gamma(b_1)\Gamma(b_2)}{\Gamma(a)\sqrt{\pi}} \int_0^1 G_{2,2}^{2,0}\left([b_1, b_2], \left[a, \frac{1}{2}\right], u\right)$$
$$\cos\left(2\sqrt{ru}\right)\frac{du}{u},$$

holds for all $r > 0$, where G denotes the Meijer-G function, generally defined through the so-called Mellin–Barnes type integral (Luke 1969, equation (1), section 5.2)) as

$$G_{p,q}^{m,n}\left([a_1, \dots, a_p], [b_1, \dots, b_q], z\right)$$
$$= \frac{1}{2\pi i} \int_L \frac{\prod_{j=1}^m \Gamma(b_j - s) \prod_{j=1}^n \Gamma(1 - a_j + s)}{\prod_{j=m+1}^q \Gamma(1 - b_j + s) \prod_{j=n+1}^p \Gamma(a_j - s)} z^s \, ds.$$

This representation holds if $z \ne 0$, $0 \le m \le q$ and $0 \le n \le p$, for integers m, n, p, q, and $a_k - b_j \ne 1, 2, 3, \dots$, for $k = 1, 2, \dots, n$ and $j = 1, 2, \dots, m$. The last constraint is set to prevent any pole of any $\Gamma(b_j - s), j = 1, 2, \dots, m$, from coinciding with any pole of any $\Gamma(1 - a_k + s), k = 1, 2, \dots, n$. With $a > 0$, $b_2 = 1 + a$ and $b_1 = \frac{1}{2}$, since $G_{2,2}^{2,0}([\frac{1}{2}, a+1], [a, \frac{1}{2}], u) = u^a$, we can therefore write

$$\int_0^1 u^{a-1} \cos\left(2\sqrt{ru}\right) du = \frac{1}{a} {}_1F_2\left(a; \frac{1}{2}, a+1; -r\right). \quad (A9)$$

Similarly, using integration by parts and properties of generalized Hypergeometric functions,

$$\int_0^1 u^{a-1} \sin\left(2\sqrt{ru}\right) du \quad (A.31)$$

$$= \frac{\sin(2\sqrt{r})}{a} - \frac{\sqrt{r}}{a} \int_0^1 u^{a-\frac{1}{2}} \cos(2\sqrt{ru}) du$$

$$= \frac{\sin(2\sqrt{r})}{a} - \frac{\sqrt{r}}{a(a+\frac{1}{2})} {}_1F_2\left(a + \frac{1}{2}; \frac{1}{2}, a + \frac{3}{2}; -r\right)$$

$$= \frac{2\sqrt{r}}{a+\frac{1}{2}} {}_1F_2\left(a + \frac{1}{2}; \frac{3}{2}, a + \frac{3}{2}; -r\right), \quad (A10)$$

where the last step follows from the definition of generalized sine function $\sin(z) = z \, {}_0F_1(\frac{3}{2}, -\frac{1}{4}z^2)$. Indeed, exploiting (6), we have

$$\frac{\sin(2\sqrt{r})}{a} - \frac{\sqrt{r}}{a(a+\frac{1}{2})} {}_1F_2\left(a + \frac{1}{2}; \frac{1}{2}, a + \frac{3}{2}; -r\right)$$

$$= \frac{2\sqrt{r}}{a} {}_0F_1\left(\frac{3}{2}, -r\right) - \frac{\sqrt{r}}{a(a+\frac{1}{2})} {}_1F_2\left(a + \frac{1}{2}; \frac{1}{2}, a + \frac{3}{2}; -r\right)$$

$$= \frac{2\sqrt{r}}{a\left(a+\frac{1}{2}\right)} \left[\left(a + \frac{1}{2}\right) {}_0F_1\left(\frac{3}{2}; -r\right)\right.$$
$$\left. - \frac{1}{2} {}_1F_2\left(a + \frac{1}{2}; \frac{1}{2}, a + \frac{3}{2}; -r\right)\right]$$

$$= \frac{2\sqrt{r}}{a\left(a+\frac{1}{2}\right)} \left[\left(a + \frac{1}{2}\right) \sum_{k=0}^{\infty} \frac{(-r)^k}{k!(3/2)_k}\right.$$
$$\left. - \frac{1}{2} \sum_{k=0}^{\infty} \frac{(a+1/2)_k}{k!(1/2)_k(a+3/2)_k}(-r)^k\right]$$

$$= \frac{2\sqrt{r}}{a\left(a+\frac{1}{2}\right)} \sum_{k=0}^{\infty} \frac{1}{k!} \left[\frac{(a+1/2)}{(3/2)_k} - \frac{1/2(a+1/2)_k}{(1/2)_k(a+3/2)_k}\right](-r)^k$$

$$= \frac{2\sqrt{r}}{a\left(a+\frac{1}{2}\right)} \sum_{k=0}^{\infty} \frac{1}{k!} \left[\frac{a(a+1/2)_k}{(3/2)_k(a+3/2)_k}\right](-r)^k$$

$$= \frac{2\sqrt{r}}{\left(a+\frac{1}{2}\right)} \sum_{k=0}^{\infty} \frac{1}{k!} \frac{(a+1/2)_k}{(3/2)_k(a+3/2)_k}(-r)^k$$

$$= \frac{2\sqrt{r}}{\left(a+\frac{1}{2}\right)} {}_1F_2\left(a + \frac{1}{2}; \frac{3}{2}, a + \frac{3}{2}; -r\right).$$

Letting $\alpha := H - \frac{1}{2}$, $\tau := t - T$, and mapping $v := t - u$, $w := \frac{v}{t}$ and $y := w^2$, we write

$$\int_0^T (t-u)^\alpha e^{i\pi u} \, du$$

$$= e^{i\pi t} \int_{(t-T)}^t v^\alpha e^{-i\pi v} \, dv$$

$$= e^{i\pi t} \left[\int_0^t v^\alpha e^{-i\pi v} \, dv - \int_0^\tau v^\alpha e^{-i\pi v} \, dv\right]$$

$$= e^{i\pi t} \left[t^{1+\alpha} \int_0^1 w^\alpha e^{-i\pi wt} \, dw - \tau^{1+\alpha} \int_0^1 w^\alpha e^{-i\pi w\tau} \, dw\right]$$

$$= \frac{e^{i\pi t}}{2} \left[t^{1+\alpha} \int_0^1 y^{\frac{\alpha-1}{2}} e^{-i\pi t\sqrt{y}} \, dy - \tau^{1+\alpha} \int_0^1 y^{\frac{\alpha-1}{2}} e^{-i\pi y\tau\sqrt{y}} \, dy\right]$$

$$= \frac{e^{i\pi t}}{2} [I(t) - I(\tau)], \quad (A11)$$

where $I(z) := z^{1+\alpha} \int_0^1 v^{\frac{\alpha-1}{2}} e^{-i\pi z\sqrt{v}} \, dv$.

We therefore write, for $z \in \{t, \tau\}$, using (A9)–(A10), $\pi z = 2\sqrt{r}$, and identifying $a - 1 = \frac{\alpha-1}{2}$,

$$I(z) = z^{1+\alpha} \int_0^1 v^{\frac{\alpha-1}{2}} e^{-i\pi z\sqrt{v}} \, dv$$

$$= z^{1+\alpha} \int_0^1 v^{\frac{\alpha-1}{2}} \cos(\pi z\sqrt{v}) \, dv - i z^{1+\alpha} \int_0^1 v^{\frac{\alpha-1}{2}} \sin(\pi z\sqrt{v}) \, dv$$

$$= \frac{2z^{1+\alpha}}{H_+} {}_1F_2\left(\frac{H_+}{2}; \frac{1}{2}, 1 + \frac{H_+}{2}; -r\right)$$

$$- i z^{H_+} \frac{4\sqrt{r}}{1 + H_+} {}_1F_2\left(\frac{1}{2} + \frac{H_+}{2}; \frac{3}{2}, \frac{3}{2} + \frac{H_+}{2}; -r\right)$$

$$= \frac{z^{H_+}}{h_1} {}_1F_2\left(h_1; \frac{1}{2}, 1+h_1; -\frac{\pi^2 z^2}{4}\right)$$

$$- i\frac{\pi z^{1+H_+}}{h_2} {}_1F_2\left(h_2; \frac{3}{2}, 1+h_2; -\frac{\pi^2 z^2}{4}\right),$$

since $\alpha = H - \frac{1}{2} = H_+ - 1$, $h_1 = \frac{H_+}{2}$ and $h_2 = \frac{1}{2} + h_1$. Plugging these into (A11), we obtain

$$\int_0^T (t-u)^\alpha e^{i\pi u}\, du$$

$$= \frac{e^{i\pi t}}{2}[I(t) - I(\tau)]$$

$$= \frac{e^{i\pi t}}{2}\left[\frac{z^{H_+}}{h_1} {}_1F_2\left(h_1; \frac{1}{2}, 1+h_1; -\frac{\pi^2 z^2}{4}\right)\right.$$

$$\left. - i\frac{\pi z^{1+H_+}}{h_2} {}_1F_2\left(h_2; \frac{3}{2}, 1+h_2; -\frac{\pi^2 z^2}{4}\right)\right]_{z=t}$$

$$- \frac{e^{i\pi t}}{2}\left[\frac{z^{H_+}}{h_1} {}_1F_2\left(h_1; \frac{1}{2}, 1+h_1; -\frac{\pi^2 z^2}{4}\right)\right.$$

$$\left. - i\frac{\pi z^{1+H_+}}{h_2} {}_1F_2\left(h_2; \frac{3}{2}, 1+h_2; -\frac{\pi^2 z^2}{4}\right)\right]_{z=\tau}$$

$$= \frac{e^{i\pi t}}{2h_1}\left[(t)^{H_+} {}_1F_2\left(h_1; \frac{1}{2}, 1+h_1; -\frac{\pi^2 t^2}{4}\right)\right.$$

$$\left. - (\tau)^{H_+} {}_1F_2\left(h_1; \frac{1}{2}, 1+h_1; -\frac{\pi^2 \tau^2}{4}\right)\right]$$

$$- i\frac{\pi e^{i\pi t}}{2h_2}\left[(t)^{1+H_+} {}_1F_2\left(h_2; \frac{3}{2}, 1+h_2; -\frac{\pi^2 t^2}{4}\right)\right.$$

$$\left. - (\tau)^{1+H_+} {}_1F_2\left(h_2; \frac{3}{2}, 1+h_2; -\frac{\pi^2 \tau^2}{4}\right)\right]$$

$$= e^{i\pi t}\left[\zeta_{\frac{1}{2}}(t, h_1) - \zeta_{\frac{1}{2}}(\tau, h_1)\right.$$

$$\left. - i\pi\left(\zeta_{\frac{3}{2}}(t, h_2) - \zeta_{\frac{3}{2}}(\tau, h_2)\right)\right],$$

where $\chi(z) := -\frac{1}{4}\pi^2 z^2$ and $\zeta_{\frac{1}{2}}$ and $\zeta_{\frac{3}{2}}$ as defined in the lemma.

A.4. *Proof of lemma 4.4*

We first prove (A). For each $n \in \mathbb{N}$ and all $t \in [T, 1]$, recall that

$$\mathcal{K}_H^T[\psi_n](t) = \sqrt{2}\int_0^T (t-u)^{H-\frac{1}{2}}\cos\left(\frac{u}{\sqrt{\lambda_n}}\right) du$$

$$= \sqrt{2}\int_{t-T}^t v^{H-\frac{1}{2}}\cos\left(\frac{t-v}{\sqrt{\lambda_n}}\right) dv,$$

with the change of variables $v = t - u$. Assume $T \leq s < t \leq 1$. Two situations are possible:

- If $0 \leq s - T < t - T \leq s < t \leq 1$, we have

$$\left|\mathcal{K}_H^T[\psi_n](t) - \mathcal{K}_H^T[\psi_n](s)\right|$$

$$= \sqrt{2}\left|\int_{t-T}^t v^{H-\frac{1}{2}}\cos\left(\frac{t-v}{\sqrt{\lambda_n}}\right) dv\right.$$

$$\left. - \int_{s-T}^s v^{H-\frac{1}{2}}\cos\left(\frac{s-v}{\sqrt{\lambda_n}}\right) dv\right|$$

$$\leq \sqrt{2}\left(\left|\int_{t-T}^s v^{H-\frac{1}{2}}\left(\cos\left(\frac{t-v}{\sqrt{\lambda_n}}\right)\right.\right.\right.$$

$$\left.\left.\left. - \cos\left(\frac{s-v}{\sqrt{\lambda_n}}\right)\right) dv\right|\right.$$

$$+ \left|\int_s^t v^{H-\frac{1}{2}}\cos\left(\frac{t-v}{\sqrt{\lambda_n}}\right) dv\right|$$

$$\left. + \left|\int_{s-T}^{t-T} v^{H-\frac{1}{2}}\cos\left(\frac{s-v}{\sqrt{\lambda_n}}\right) dv\right|\right)$$

$$\leq \sqrt{2}\left(\int_{t-T}^s v^{H-\frac{1}{2}}\left|\cos\left(\frac{t-v}{\sqrt{\lambda_n}}\right) - \cos\left(\frac{s-v}{\sqrt{\lambda_n}}\right)\right| dv\right.$$

$$\left. + \int_s^t v^{H-\frac{1}{2}} dv + \int_{s-T}^{t-T} v^{H-\frac{1}{2}} dv\right)$$

$$\leq \sqrt{2}\left(\int_{t-T}^s v^{H-\frac{1}{2}}\left|\frac{t-s}{\sqrt{\lambda_n}}\right| dv\right.$$

$$\left. + K|t-s|^{H+\frac{1}{2}} + K|t-s|^{H+\frac{1}{2}}\right)$$

$$\leq \sqrt{2}\left(\frac{|t-s|}{\sqrt{\lambda_n}}\int_{t-T}^s v^{H-\frac{1}{2}} dv + 2K|t-s|^{H+\frac{1}{2}}\right)$$

$$\leq \sqrt{2}\left(\frac{|t-s|}{\sqrt{\lambda_n}}\|(\cdot)^{H-\frac{1}{2}}\|_{L^1[0,1]} + 2K|t-s|^{H+\frac{1}{2}}\right)$$

$$\leq \widetilde{C}_1^T |t-s|^{H+\frac{1}{2}},$$

with $\widetilde{C}_1^T = \max\{2\sqrt{2}K, \sqrt{\frac{2}{\lambda_n}}\|(\cdot)^{H-\frac{1}{2}}\|_{L^1[0,1]}\} = \max\{2\sqrt{2}K, \frac{\sqrt{2}(2n-1)\pi}{2}\|(\cdot)^{H-\frac{1}{2}}\|_{L^1[0,1]}\}$, since $\cos(\cdot)$ is Lipschitz on any compact and $\int_0^{\cdot} v^{H-\frac{1}{2}} dv$ is $(H+\frac{1}{2})$-Hölder continuous.

- If $0 \leq s - T \leq s \leq t - T \leq t \leq 1$,

$$\left|\mathcal{K}_H^T[\psi_n](t) - \mathcal{K}_H^T[\psi_n](s)\right|$$

$$= \sqrt{2}\left|\int_{t-T}^t v^{H-\frac{1}{2}}\cos\left(\frac{t-v}{\sqrt{\lambda_n}}\right) dv\right.$$

$$\left. - \int_{s-T}^s v^{H-\frac{1}{2}}\cos\left(\frac{s-v}{\sqrt{\lambda_n}}\right) dv\right|$$

$$= \sqrt{2}\left|\int_{t-T}^t v^{H-\frac{1}{2}}\cos\left(\frac{t-v}{\sqrt{\lambda_n}}\right) dv\right.$$

$$- \int_{s-T}^s v^{H-\frac{1}{2}}\cos\left(\frac{s-v}{\sqrt{\lambda_n}}\right) dv$$

$$+ \int_s^{t-T} v^{H-\frac{1}{2}}\cos\left(\frac{t-v}{\sqrt{\lambda_n}}\right) dv$$

$$- \int_s^{t-T} v^{H-\frac{1}{2}}\cos\left(\frac{t-v}{\sqrt{\lambda_n}}\right) dv$$

$$+ \int_s^{t-T} v^{H-\frac{1}{2}}\cos\left(\frac{s-v}{\sqrt{\lambda_n}}\right) dv$$

$$\left. - \int_s^{t-T} v^{H-\frac{1}{2}}\cos\left(\frac{s-v}{\sqrt{\lambda_n}}\right) dv\right|$$

$$\leq \sqrt{2}\left(\left|\int_s^{t-T} v^{H-\frac{1}{2}}\left(\cos\left(\frac{t-v}{\sqrt{\lambda_n}}\right)\right.\right.\right.$$

$$\left.\left.\left. - \cos\left(\frac{s-v}{\sqrt{\lambda_n}}\right)\right) dv\right|\right.$$

$$\left. + \left|\int_s^t v^{H-\frac{1}{2}}\cos\left(\frac{t-v}{\sqrt{\lambda_n}}\right) dv\right|\right.$$

$$+ \left| \int_{s-T}^{t-T} v^{H-\frac{1}{2}} \cos\left(\frac{s-v}{\sqrt{\lambda_n}}\right) dv \right| \right)$$

$$\leq \cdots \leq \widetilde{C}_1^T |t-s|^{H+\frac{1}{2}},$$

where the dots correspond to the same computations as in the previous case and leads to the same estimation with the same constant $\widetilde{C}_1^T$.

This proves (A).

To prove (B), recall that, for $T \in [0,1]$ and $n \in \mathbb{N}$, the function $\mathcal{K}_H^T[\psi_n] : [T,1] \to \mathbb{R}$ reads

$$\mathcal{K}_H^T[\psi_n](t) = \sqrt{2} \int_0^T (t-s)^{H-\frac{1}{2}} \cos\left(\left(n-\frac{1}{2}\right)\pi s\right) ds$$

$$= \frac{\sqrt{2}}{m^{H+\frac{1}{2}}} \int_0^{mT} (mt-u)^{H-\frac{1}{2}} \cos(\pi u) \, du =: \Phi_m(t).$$
(A12)

with the change of variable $u = (n-\frac{1}{2})s =: ms$. Denote from now on $\widetilde{\mathbb{N}} := \{m = n - \frac{1}{2}, n \in \mathbb{N}\}$. From (A12), we deduce, for each $m \in \widetilde{\mathbb{N}}$ and $t \in [T,1]$,

$$m^{H+\frac{1}{2}} \Phi_m(t) = \sqrt{2} \int_0^{mT} (mt-u)^{H-\frac{1}{2}} \cos(\pi u) \, du =: \sqrt{2}\phi_m(t).$$
(A13)

To end the proof of (B), it therefore suffices to show that $(\phi_m(t))_{m \in \widetilde{\mathbb{N}}, t \in [T,1]}$ is uniformly bounded since, in that case we have

$$\|\mathcal{K}_H^T[\psi_n]\|_\infty = \sup_{t \in [T,1]} |\mathcal{K}_H^T[\psi_n](t)|$$

$$= \sup_{t \in [T,1]} |\Phi_{n-\frac{1}{2}}(t)|$$

$$= \frac{\sqrt{2}}{(n-\frac{1}{2})^{H+\frac{1}{2}}} \sup_{t \in [T,1]} |\phi_{n-\frac{1}{2}}(t)|$$

$$\leq \frac{\sqrt{2}}{(n-\frac{1}{2})^{H+\frac{1}{2}}} \sup_{t \in [T,1], m \in \widetilde{\mathbb{N}}} |\phi_m(t)|$$

$$\leq \frac{\sqrt{2}}{(n-\frac{1}{2})^{H+\frac{1}{2}}} C \leq C_2^T n^{-(H+\frac{1}{2})},$$

for some $C_2^T > 0$, proving (B). The following guarantees the uniform boundedness of ϕ_x in (A13).

PROPOSITION A.4.1 *For any $T \in [0,1]$, there exists $C > 0$ such that $|\phi_x(t)| \leq C$ for all $x \geq 0$, $t \in [T,1]$.*

Proof For $x > 0$, we write

$$\phi_x(t) = \int_0^{xT} (xt-u)^{H-\frac{1}{2}} \cos(\pi u) \, du$$

$$= \Re\left\{ \int_0^{xT} (xt-u)^{H-\frac{1}{2}} e^{i\pi u} \, du \right\}.$$

Using the representation in lemma 4.5, we are thus left to prove that the maps $\zeta_{\frac{1}{2}}(\cdot, h_1)$ and $\zeta_{\frac{3}{2}}(\cdot, h_2)$, defined in (13), are bounded on $[0,\infty)$ by, say $L_{\frac{1}{2}}$ and $L_{\frac{3}{2}}$. Indeed, in this case,

$$\sup_{x>0, t \in [T,1]} |\phi_x(t)|$$

$$= \sup_{x>0, t \in [T,1]} \left| \int_0^{xT} (xt-u)^{H-\frac{1}{2}} e^{i\pi u} \, du \right|$$

$$\leq \sup_{x>0, t \in [T,1]} \left| \frac{e^{i\pi xt}}{2} \left[\left(\zeta_{\frac{1}{2}}(xt, h_1) - \zeta_{\frac{1}{2}}(x(t-T), h_1) \right) \right. \right.$$

$$\left. \left. - i\pi \left(\zeta_{\frac{3}{2}}(xt, h_2) - \zeta_{\frac{3}{2}}(x(t-T), h_2) \right) \right] \right|$$

$$\leq \frac{1}{2} \sup_{y,z \in [0,\infty)} \left| \left(\zeta_{\frac{1}{2}}(y, h_1) - \zeta_{\frac{1}{2}}(z, h_1) \right) \right.$$

$$\left. - i\pi \left(\zeta_{\frac{3}{2}}(y, h_2) - \zeta_{\frac{3}{2}}(z, h_2) \right) \right|$$

$$\leq \pi \left\{ \sup_{y \in [0,\infty)} \left| \zeta_{\frac{1}{2}}(y, h_1) \right| + \sup_{y \in [0,\infty)} \left| \zeta_{\frac{3}{2}}(y, h_2) \right| \right\}$$

$$\leq L_{\frac{1}{2}} + L_{\frac{3}{2}} = C < +\infty.$$

The maps $\zeta_{\frac{1}{2}}(\cdot, h_1)$ and $\zeta_{\frac{3}{2}}(\cdot, h_2)$ are both clearly continuous. Moreover, as z tends to infinity $\zeta_k(z, h)$ converges to a constant c_k, for $(k,h) \in (\{\frac{1}{2}, \frac{3}{2}\}, \{h_1, h_2\})$. The identities

$$\frac{{}_1F_2\left(h; \frac{1}{2}, 1+h; -x\right)}{h} = \int_0^1 \frac{\cos(2\sqrt{xu})}{u^{1-h}} \, du \quad \text{and}$$

$$\frac{{}_1F_2\left(h; \frac{3}{2}, 1+h; -x\right)}{h} = \frac{1}{2\sqrt{x}} \int_0^1 \frac{\sin(2\sqrt{xu})}{u^{3/2-h}} \, du$$

hold (this can be checked with `Wolfram Mathematica` for example) and therefore,

$$\zeta_{\frac{1}{2}}(z, h_1) = \frac{z^{2h_1}}{2h_1} {}_1F_2\left(h_1; \frac{1}{2}, 1+h_1; -\frac{\pi^2 z^2}{4}\right)$$

$$= \frac{z^{2h_1}}{2} \int_0^1 u^{h_1-1} \cos(\pi z \sqrt{u}) \, du$$

$$= \frac{z^{2h_1}}{2} \int_0^{\pi z} \frac{x^{2(h_1-1)}}{(\pi z)^{2(h_1-1)}} \cos(x) \frac{2x}{\pi^2 z^2} \, dx$$

$$= \frac{1}{\pi^{2h_1}} \int_0^{\pi z} x^{2h_1-1} \cos(x) \, dx,$$

where, in the second line, we used the change of variables $x = \pi z \sqrt{u}$. In particular, as z tends to infinity, this converges to $\pi^{-2h_1} \int_0^{+\infty} x^{2h_1-1} \cos(x) \, dx = \frac{\cos(\pi h_1)}{\pi^{2h_1}} \Gamma(2h_1) =: c_{1/2} \approx 0.440433$. Analogously, for $k = \frac{3}{2}$,

$$\zeta_{\frac{3}{2}}(z, h_2) = \frac{z^{2h_2}}{2h_2} {}_1F_2\left(h_2; \frac{3}{2}, 1+h_2; -\frac{\pi^2 z^2}{4}\right)$$

$$= \frac{z^{2h_2}}{2\pi z} \int_0^1 u^{h_2-3/2} \sin(\pi z \sqrt{u}) \, du$$

$$= \frac{z^{2h_2-1}}{2\pi} \int_0^{\pi z} \frac{x^{2h_2-3)}}{(\pi z)^{2h_2-3)}} \sin(x) \frac{2x}{\pi^2 z^2} \, dx$$

$$= \frac{1}{\pi^{2h_2}} \int_0^{\pi z} x^{2(h_2-1)} \sin(x) \, dx,$$

with the same change of variables as before. This converges to $\pi^{-2h_2} \int_0^{+\infty} x^{2h_2-2} \sin(x) \, dx = \frac{-\cos(\pi h_2)}{\pi^{2h_2}} \Gamma(2h_2-1) =: c_{3/2} \approx 0.193$ as z tends to infinity. For $k > 0$, $\zeta_k(z, h) = z^{2h}(1 + \mathcal{O}(z^2))$ at zero. Since $H \in (0, \frac{1}{2})$, the two functions are continuous and bounded and the proposition follows. ∎

A.5. *Proof of theorem 4.11*

We only provide the proof of (15) since, as already noticed, that of (16) follows immediately. Suppose that $F : \mathbb{R} \to \mathbb{R}$ is Lipschitz continuous with constant M. By definitions (11) and (14), we have

$$\left| \mathbb{E}[F(\text{VIX}_T)] - \mathbb{E}\left[F\left(\widehat{\text{VIX}}_T^{\mathbf{d}}\right)\right] \right|$$

$$= \left| \mathbb{E}\left[F\left(\left| \frac{1}{\Delta} \int_T^{T+\Delta} v_0(t) \exp\left\{ \gamma Z_t^{T,\Delta} \right.\right.\right.\right.\right.$$
$$\left.\left.\left.\left. + \frac{\gamma^2}{2}\left(\int_0^{t-T} K(s)^2 \, ds - \int_0^t K(s)^2 \, ds \right) \right\} dt \right|^{\frac{1}{2}} \right) \right]$$
$$- \mathbb{E}\left[F\left(\left| \frac{1}{\Delta} \int_T^{T+\Delta} v_0(t) \exp\left\{ \gamma \widehat{Z}_t^{T,\Delta,\mathbf{d}} \right.\right.\right.\right.$$
$$\left.\left.\left.\left.\left. + \frac{\gamma^2}{2}\left(\int_0^{t-T} K(s)^2 \, ds - \int_0^t K(s)^2 \, ds \right) \right\} dt \right|^{\frac{1}{2}} \right) \right] \right|.$$

For clarity, let $Z := Z^{T,\Delta}$, $\widehat{Z} := \widehat{Z}^{T,\Delta,\mathbf{d}}$, $\mathfrak{H} := \int_T^{T+\Delta} h(t) e^{\gamma Z_t} \, dt$ and $\widehat{\mathfrak{H}} := \int_T^{T+\Delta} h(t) e^{\gamma \widehat{Z}_t} \, dt$, with

$$h(t) := \frac{v_0(t)}{\Delta} \exp\left\{ \frac{\gamma^2}{2}\left(\int_0^{t-T} K(s)^2 \, ds - \int_0^t K(s)^2 \, ds \right) \right\},$$
$$\text{for } t \in [T, T+\Delta].$$

We can therefore write, using the Lipschitz property of F (with constant M) and lemma A.4,

$$\left| \mathbb{E}\left[F\left(\mathrm{VIX}_T \right) \right] - \mathbb{E}\left[F\left(\widehat{\mathrm{VIX}}_T^{\mathbf{d}} \right) \right] \right|$$
$$= \left| \mathbb{E}\left[F\left(\mathfrak{H}^{\frac{1}{2}} \right) \right] - \mathbb{E}\left[F\left(\widehat{\mathfrak{H}}^{\frac{1}{2}} \right) \right] \right| \le \mathbb{E}\left[\left| F\left(\mathfrak{H}^{\frac{1}{2}} \right) - F\left(\widehat{\mathfrak{H}}^{\frac{1}{2}} \right) \right| \right]$$
$$\le M \mathbb{E}\left[\left| \mathfrak{H}^{\frac{1}{2}} - \widehat{\mathfrak{H}}^{\frac{1}{2}} \right| \right] \le M \mathbb{E}\left[\left(\frac{1}{\mathfrak{H}} + \frac{1}{\widehat{\mathfrak{H}}} \right) \left| \mathfrak{H} - \widehat{\mathfrak{H}} \right| \right]$$
$$=: M \mathbb{E}\left[A \left| \mathfrak{H} - \widehat{\mathfrak{H}} \right| \right] \le M \mathbb{E}\left[A \int_T^{T+\Delta} h(t) \left| e^{\gamma Z_t} - e^{\gamma \widehat{Z}_t} \right| dt \right]$$
$$\le M \mathbb{E}\left[A \int_T^{T+\Delta} h(t)\gamma \left(e^{\gamma Z_t} + e^{\gamma \widehat{Z}_t} \right) \left| Z_t - \widehat{Z}_t \right| dt \right].$$

Now, an application of Hölder's inequality yields

$$\left| \mathbb{E}\left[F\left(\mathrm{VIX}_T \right) \right] - \mathbb{E}\left[F\left(\widehat{\mathrm{VIX}}_T^{\mathbf{d}} \right) \right] \right|$$
$$\le M \mathbb{E}\left[\gamma A \left| \int_T^{T+\Delta} h(t)^2 \left(e^{\gamma Z_t} + e^{\gamma \widehat{Z}_t} \right)^2 dt \right|^{\frac{1}{2}} \right.$$
$$\left. \times \left| \int_T^{T+\Delta} \left| Z_t - \widehat{Z}_t \right|^2 dt \right|^{\frac{1}{2}} \right]$$
$$\le M \mathbb{E}\left[(\gamma A)^2 \int_T^{T+\Delta} h(t)^2 \left(e^{\gamma Z_t} + e^{\gamma \widehat{Z}_t} \right)^2 dt \right]^{\frac{1}{2}}$$
$$\times \mathbb{E}\left[\int_T^{T+\Delta} \left| Z_t - \widehat{Z}_t \right|^2 dt \right]^{\frac{1}{2}}$$
$$= \mathfrak{K} \, \mathbb{E}\left[\int_T^{T+\Delta} \left| Z_t - \widehat{Z}_t \right|^2 dt \right]^{\frac{1}{2}},$$

where $\mathfrak{K} := M \mathbb{E}[\gamma^2 A^2 \int_T^{T+\Delta} h(t)^2 (e^{\gamma Z_t} + e^{\gamma \widehat{Z}_t})^2 \, dt]^{\frac{1}{2}}$. It remains to show that $\mathfrak{K}$ is a strictly positive finite constant. This follows from the fact that $\{Z_t\}_{t\in[T,T+\Delta]}$ does not explode in finite time (and so does not its quantization $\widehat{Z}$ either). The identity $(a+b)^2 \le 2(a^2+b^2)$ and Hölder's inequality imply

$$\mathfrak{K}^2 \le 4M^2\gamma^2 \mathbb{E}\left[\left(\frac{1}{\mathfrak{H}} + \frac{1}{\widehat{\mathfrak{H}}} \right) \int_T^{T+\Delta} h(t)^2 \left(e^{2\gamma Z_t} + e^{2\gamma \widehat{Z}_t} \right) dt \right]$$
$$\le 4M^2\gamma^2 \mathbb{E}\left[\left| \frac{1}{\mathfrak{H}} + \frac{1}{\widehat{\mathfrak{H}}} \right|^2 \right]^{\frac{1}{2}}$$

$$\times \mathbb{E}\left[\left| \int_T^{T+\Delta} h(t)^2 \left(e^{2\gamma Z_t} + e^{2\gamma \widehat{Z}_t} \right) dt \right|^2 \right]^{\frac{1}{2}}$$
$$\le 16M^2\gamma^2 \mathbb{E}\left[\frac{1}{\mathfrak{H}^2} + \frac{1}{\widehat{\mathfrak{H}}^2} \right]^{\frac{1}{2}}$$
$$\times \mathbb{E}\left[\left| \int_T^{T+\Delta} h(t)^2 e^{2\gamma Z_t} dt \right|^2 + \left| \int_T^{T+\Delta} h(t)^2 e^{2\gamma \widehat{Z}_t} dt \right|^2 \right]^{\frac{1}{2}}$$
$$=: 16M^2\gamma^2 (A_1 + A_2)^{\frac{1}{2}} (B_1 + B_2)^{\frac{1}{2}}.$$

We only need to show that A_1, A_2, B_1 and B_2 are finite. Since h is a positive continuous function on the compact interval $[T, T+\Delta]$, we have

$$\mathfrak{H} \ge \int_T^{T+\Delta} \inf_{s\in[T,T+\Delta]} \left(h(s) e^{\gamma Z_s} \right) dt \ge \Delta \inf_{s\in[T,T+\Delta]} h(s) e^{\gamma Z_s}$$
$$\ge \Delta \inf_{t\in[T,T+\Delta]} h(t) \inf_{s\in[T,T+\Delta]} e^{\gamma Z_s} \ge \Delta \widetilde{h} \exp\left\{ \gamma \inf_{s\in[T,T+\Delta]} Z_s \right\}, \tag{A14}$$

with $\widetilde{h} := \inf_{t\in[T,T+\Delta]} h(t) > 0$. The inequality (A14) implies

$$A_1 = \mathbb{E}\left[\mathfrak{H}^{-2} \right] \le \frac{\mathbb{E}\left[\exp\left\{ -2\gamma \inf_{s\in[T,T+\Delta]} Z_s \right\} \right]}{\Delta^2 \widetilde{h}^2}$$
$$= \frac{\mathbb{E}\left[\exp\left\{ 2\gamma \sup_{s\in[T,T+\Delta]} (-Z_s) \right\} \right]}{\Delta^2 \widetilde{h}^2}$$
$$= \frac{1}{\Delta^2 \widetilde{h}^2} \mathbb{E}\left[\exp\left\{ 2\gamma \sup_{s\in[T,T+\Delta]} Z_s \right\} \right],$$

since $-Z$ and Z have the same law. The process $Z = (Z_t)_{t\in[T,T+\Delta]}$ is a continuous centered Gaussian process defined on a compact set. Thus, by theorem 1.5.4 in Adler and Taylor (2007), it is almost surely bounded there. Furthermore, exploiting Lemma A.5 and *Borel-TIS* inequality (Adler and Taylor 2007, Theorem 2.1.1), we have

$$\mathbb{E}\left[e^{2\gamma \sup_{s\in[T,T+\Delta]} Z_s} \right] =: \mathbb{E}\left[e^{2\gamma \|Z\|} \right] = \int_0^{+\infty} \mathbb{P}\left(e^{2\gamma \|Z\|} > u \right) du$$
$$= \int_0^{+\infty} \mathbb{P}\left(\|Z\| > \frac{\log(u)}{2\gamma} \right) du$$
$$= \int_0^{e^{2\gamma \mathbb{E}[\|Z\|]}} du + \int_{e^{2\gamma \mathbb{E}[\|V\|]}}^{+\infty} \mathbb{P}\left(\|Z\| > \frac{\log(u)}{2\gamma} \right) du$$
$$= e^{2\gamma \mathbb{E}[\|Z\|]} + \int_{e^{2\gamma \mathbb{E}[\|V\|]}}^{+\infty} e^{-\frac{1}{2}\left(\frac{\frac{1}{2\gamma}\log(u) - \mathbb{E}[\|Z\|]}{\sigma_T} \right)^2} du$$
$$\le e^{2\gamma \mathbb{E}[\|Z\|]} + \int_0^{+\infty} e^{-\frac{1}{2}\left(\frac{\frac{1}{2\gamma}\log(u) - \mathbb{E}[\|Z\|]}{\sigma_T} \right)^2} du, \tag{A15}$$

with $\|Z\| := \sup_{s\in[T,T+\Delta]} Z_s$ and $\sigma_T^2 := \sup_{t\in[T,T+\Delta]} \mathbb{E}[Z_t^2]$. The change of variable $\frac{\log(u)}{2\gamma} = v$ in the last term in (A15) yields

$$\int_0^{+\infty} e^{-\frac{1}{2}\left(\frac{\frac{1}{2\gamma}\log(u) - \mathbb{E}[\|Z\|]}{\sigma_T} \right)^2} du = 2\gamma \int_{\mathbb{R}} e^{-\frac{1}{2}\left(\frac{v - \mathbb{E}[\|Z\|]}{\sigma_T} \right)^2} e^{2\gamma v} dv$$
$$= \sqrt{2\pi} \, 2\gamma \, \mathbb{E}[e^{2\gamma Y}],$$

since $Y \sim \mathcal{N}(\mathbb{E}[\|Z\|], \sigma_T)$, and hence A_1 is finite. Now, note that, in analogy to the last line of the proof of proposition 3.12, for any $t \in [T, T+\Delta]$, we have

$$\mathbb{E}\left[Z_t \middle| (\widehat{Z}_s)_{s\in[T,T+\Delta]} \right] = \mathbb{E}\left[\mathbb{E}\left[Z_t \middle| \{\widehat{\xi}_n^{d(n)}\}_{n=1,\dots,m} \right] \middle| (\widehat{Z}_s)_{s\in[T,T+\Delta]} \right]$$
$$= \mathbb{E}\left[\widehat{Z}_t \middle| (\widehat{Z}_s)_{s\in[T,T+\Delta]} \right] = \widehat{Z}_t, \tag{A16}$$

since the sigma-algebra generated by $(\widehat{Z}_s)_{s\in[T,T+\Delta]}$ is included in the sigma-algebra generated by $\{\widehat{\xi}_n^{d(n)}\}_{n=1,\ldots,m}$. Now, exploiting, in sequence, (A16), the conditional version of $\sup_{t\in[T_1,T_2]}\mathbb{E}[f_t] \le \mathbb{E}[\sup_{t\in[T_1,T_2]}f_t]$, conditional Jensen's inequality together with the convexity of $x \mapsto e^{\gamma x}$, for $\gamma > 0$ and the tower property, we obtain

$$\mathbb{E}\left[\exp\left\{\gamma \sup_{t\in[T,T+\Delta]} \widehat{Z}_t\right\}\right]$$

$$= \mathbb{E}\left[\exp\left\{\gamma \sup_{t\in[T,T+\Delta]} \mathbb{E}\left[Z_t\big|(\widehat{Z}_s)_{s\in[T,T+\Delta]}\right]\right\}\right]$$

$$\le \mathbb{E}\left[\exp\left\{\gamma \mathbb{E}\left[\sup_{t\in[T,T+\Delta]} Z_t\big|(\widehat{Z}_s)_{s\in[T,T+\Delta]}\right]\right\}\right]$$

$$\le \mathbb{E}\left[\mathbb{E}\left[\exp\left\{\gamma \sup_{t\in[T,T+\Delta]} Z_t\right\}\big|(\widehat{Z}_s)_{s\in[T,T+\Delta]}\right]\right]$$

$$= \mathbb{E}\left[\exp\left\{\gamma \sup_{t\in[T,T+\Delta]} Z_t\right\}\right].$$

Thus we have

$$A_2 = \mathbb{E}\left[\widehat{\mathfrak{H}}^{-2}\right] \le \frac{1}{\Delta^2\widetilde{h}^2}\mathbb{E}\left[\exp\left\{\gamma \sup_{t\in[T,T+\Delta]} \widehat{Z}_t\right\}\right]$$

$$s \le \frac{1}{\Delta^2\widetilde{h}^2}\mathbb{E}\left[\exp\left\{\gamma \sup_{t\in[T,T+\Delta]} Z_t\right\}\right],$$

which is finite because of the proof of the finiteness of A_1, above.

Exploiting Fubini's theorem we rewrite B_1 as

$$B_1 = \mathbb{E}\left[\left(\int_T^{T+\Delta} h(t)^2 e^{2\gamma Z_t}\,\mathrm{d}t\right)^2\right]$$

$$= \int_T^{T+\Delta}\int_T^{T+\Delta} h(t)^2 h(s)^2 \mathbb{E}\left[e^{2\gamma(Z_t+Z_s)}\right]\mathrm{d}t\,\mathrm{d}s.$$

Since $(Z_t)_{t\in[T,T+\Delta]}$ is centered Gaussian with covariance $\mathbb{E}[Z_tZ_s] = \int_0^T K(t-u)K(s-u)\,\mathrm{d}u$, then $(Z_t + Z_s) \sim \mathcal{N}(0,g(t,s))$, with $g(t,s) := \mathbb{E}[(Z_t + Z_s)^2] = \int_0^T (K(t-u)+K(s-u))^2\,\mathrm{d}u$ and therefore

$$B_1 = \int_T^{T+\Delta}\int_T^{T+\Delta} h(t)^2 h(s)^2 e^{2\gamma^2 g(t,s)}\,\mathrm{d}t\,\mathrm{d}s$$

is finite since both h and g are continuous on compact intervals. Finally, for B_2 we have

$$B_2 = \mathbb{E}\left[\left(\int_T^{T+\Delta} h(t)^2 e^{2\gamma \widehat{Z}_t}\,\mathrm{d}t\right)^2\right]$$

$$= \int_T^{T+\Delta}\int_T^{T+\Delta} h(t)^2 h(s)^2 \mathbb{E}\left[e^{2\gamma(\widehat{Z}_t+\widehat{Z}_s)}\right]\mathrm{d}t\,\mathrm{d}s$$

$$\le \int_T^{T+\Delta}\int_T^{T+\Delta} h(t)^2 h(s)^2 \mathbb{E}\left[e^{2\gamma(Z_t+Z_s)}\right]\mathrm{d}t\,\mathrm{d}s = B_1,$$

where we have used the fact that for all $t,s \in [T,T+\Delta]$, $(\widehat{Z}_t + \widehat{Z}_s)$ is a stationary quantizer for $(Z_t + Z_s)$ and so $\mathbb{E}[e^{2\gamma(\widehat{Z}_t+\widehat{Z}_s)}] \le \mathbb{E}[e^{2\gamma(Z_t+Z_s)}]$ since $f(x) = e^{2\gamma x}$ is a convex function (see remark 3.9 in section 3.1). Therefore B_2 is finite and the proof follows.

Appendix 2. Some useful results

We recall some important results used throughout the text. Straightforward proofs are omitted.

PROPOSITION A.5.1 *For a Gaussian random variable* $Z \sim \mathcal{N}(\mu,\sigma)$,

$$\mathbb{E}\left[|Z-\mu|^p\right] = \begin{cases} (p-1)!!\sigma^p, & \text{if } p \text{ is even,} \\ 0, & \text{if } p \text{ is odd.} \end{cases}$$

We recall (Steele 2004, Problem 8.5), correcting a small error, used in the proof of Proposition 3.6:

LEMMA A.5.2 *Let* $m, N \in \mathbb{N}$ *and* $p_1,\ldots,p_m$ *positive real numbers. Then*

$$\inf\left\{\sum_{n=1}^m \frac{p_n}{x_n^2} : x_1,\ldots,x_m \in (0,\infty), \prod_{n=1}^m x_n \le N\right\}$$

$$= mN^{-\frac{2}{m}}\left(\prod_{j=1}^m p_j\right)^{\frac{1}{m}},$$

where the infimum is attained for $x_n = N^{\frac{1}{m}}p_n^{\frac{1}{2}}(\prod_{j=1}^m p_j)^{-\frac{1}{2m}}$, *for all* $n \in \{1,\ldots,m\}$.

Proof The general arithmetic-geometric inequalities imply

$$\frac{1}{m}\sum_{n=1}^m \frac{p_n}{x_n^2} \ge \left(\prod_{n=1}^m \frac{p_n}{x_n^2}\right)^{\frac{1}{m}} = \left(\prod_{n=1}^m p_n\right)^{\frac{1}{m}}\left(\prod_{n=1}^m \frac{1}{x_n^2}\right)^{\frac{1}{m}}$$

$$\ge \left(\prod_{n=1}^m p_n\right)^{\frac{1}{m}} N^{-\frac{2}{m}},$$

since $\prod_{n=1}^m x_n \ge N$ by assumption. The right-hand side does not depend on $x_1,\ldots,x_m$, so

$$\inf\left\{\sum_{n=1}^m \frac{p_n}{x_n^2} : x_1,\ldots,x_m \in (0,\infty), \prod_{n=1}^m x_n \le N\right\}$$

$$\ge m\left(\prod_{n=1}^m p_n\right)^{\frac{1}{m}} N^{-\frac{2}{m}}.$$

Choosing $\widetilde{x}_n = N^{\frac{1}{m}}p_n^{\frac{1}{2}}(\prod_{j=1}^m p_j)^{-\frac{1}{2m}}$, for all $n \in \{1,\ldots,m\}$, we obtain

$$m\left(\prod_{n=1}^m \frac{p_n}{N^2}\right)^{\frac{1}{m}} = \sum_{n=1}^m \frac{p_n}{\widetilde{x}_n^2}$$

$$\ge \inf\left\{\sum_{n=1}^m \frac{p_n}{x_n^2} : x_1,\ldots,x_m \in (0,\infty), \prod_{n=1}^m x_n \le N\right\}$$

$$\ge m\left(\prod_{n=1}^m \frac{p_n}{N^2}\right)^{\frac{1}{m}},$$

which concludes the proof. ∎

LEMMA A.5.3 *The following hold:*

(i) *For any* $x, y > 0$, $|\sqrt{x} - \sqrt{y}| \le (\frac{1}{\sqrt{x}} + \frac{1}{\sqrt{y}})|x - y|$.

(ii) *Set* $C > 0$. *For any* $x, y \in \mathbb{R}$, $|e^{Cx} - e^{Cy}| \le C(e^{Cx} + e^{Cy})|x - y|$.

LEMMA A.5.4 *For a positive random variable* X *on* $(\Omega,\mathcal{F},\mathbb{P})$, $\mathbb{E}[X] = \int_0^{+\infty} \mathbb{P}(X > u)\,\mathrm{d}u$.